Journal of Computational Physics 256 (2014) 748–767

Contents lists available at ScienceDirect

Journal of Computational Physics

www.elsevier.com/locate/jcp

Weak imposition of the slip boundary condition on curved boundaries for Stokes flow

José M. Urquiza [a,*], André Garon [b], Marie-Isabelle Farinas [c]

[a] GIREF, Département de mathématiques et de statistique, Université Laval, Québec, QC, G1V 0A6, Canada
[b] Département de Génie Mécanique, École Polytechnique de Montréal, Montréal, QC, H3T 1J4, Canada
[c] Département des sciences appliquées, Université du Québec à Chicoutimi, Chicoutimi, QC, G7H 2B1, Canada

ARTICLE INFO

Article history:
Received 16 January 2012
Received in revised form 27 April 2013
Accepted 19 August 2013
Available online 11 September 2013

Keywords:
Stokes and Navier–Stokes equations
Slip boundary conditions
Finite element method
Babuska's paradox
Lagrange multiplier method
Nitsche's method

ABSTRACT

We study the finite element approximation of two methods to weakly impose a slip boundary condition for incompressible fluid flows: the Lagrange multiplier method and Nitsche's method. For each method, we can distinguish several formulations depending on the values of some real parameters. In the case of a spatial domain with a polygonal or polyhedral boundary, we prove convergence results of their finite element approximations, extending previous results of Verfürth [33] and we show numerical results confirming them. In the case of a spatial domain with a smooth curved boundary, numerical results show that approximations computed on polygonal domains approximating the original domain may not converge to the exact solution, depending on the values of the aforementioned parameters and on the finite element discretization. These negative results seem to highlight Babuska's like paradox, due to the approximation of the boundary by polygonal ones. In particular, they seem to contradict some of Verfürth's theoretical convergence results.

1. Introduction

In Ω, an open bounded and connected subset of $\mathbf{R}^n$, $n = 2$ or 3, with Lipschitz continuous boundary $\Gamma = \partial\Omega$, we consider the stationary Stokes equations

$$-\nabla \cdot \boldsymbol{T}(\boldsymbol{u}, p) = \boldsymbol{f} \quad \text{in } \Omega, \tag{1}$$

$$\nabla \cdot \boldsymbol{u} = 0 \quad \text{in } \Omega, \tag{2}$$

where $\boldsymbol{T}(\boldsymbol{u}, p) = -p\boldsymbol{I} + 2\mu\boldsymbol{D}(\boldsymbol{u})$ is the stress tensor, $\boldsymbol{D}(\boldsymbol{u}) = (\nabla\boldsymbol{u} + \nabla\boldsymbol{u}^T)/2$ is the deformation rate tensor and $\mu > 0$ is the kinematic viscosity of the fluid. On the boundary we prescribe a *slip* boundary condition:

$$\boldsymbol{u} \cdot \boldsymbol{\nu} = g \quad \text{on } \Gamma, \tag{3}$$

$$\boldsymbol{\nu} \cdot \boldsymbol{T}(\boldsymbol{u}, p) \cdot \boldsymbol{\tau_i} = f_{2,i}, \quad i = 1, n-1, \text{ on } \Gamma. \tag{4}$$

Here, $\boldsymbol{\nu}$ is the outgoing unit normal vector to Γ whereas $\boldsymbol{\tau_i}$, $i = 1, n-1$, are orthonormal vectors spanning the plane tangent to Γ. When $g = 0$ (zero-flux condition) and $f_{2,i} = 0$, $i = 1, n-1$ (vanishing forces in tangential directions to the boundary), this is also known as the *free slip* boundary condition.

* Corresponding author.
E-mail addresses: jose.urquiza@mat.ulaval.ca (J.M. Urquiza), andre.garon@polymtl.ca (A. Garon), Marie-Isabelle_Farinas@uqac.ca (M.-I. Farinas).

0021-9991/$ – see front matter
http://dx.doi.org/10.1016/j.jcp.2013.08.045

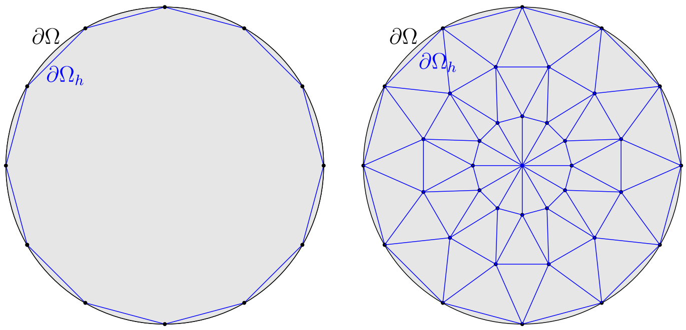

Fig. 1. Smooth domain Ω and its meshed approximation Ω_h.

In the literature, slip-type boundary conditions are less frequent than, for instance, Dirichlet or Neumann (free) boundary conditions. Nevertheless, they are involved in problems with biological surfaces and interfaces [6,7], polymer melts [13], slide coating [11], turbulence models [24], or special problems with Newtonian fluid flows at solid interfaces [25]. They can be viewed as a mix of a Dirichlet boundary condition in the normal direction to the boundary and a Neumann (*i.e. natural*) boundary condition in tangential directions.

In the numerical literature, several weak formulations have been devised to form the basis of a finite element approximation of Stokes or Navier–Stokes equations with a slip boundary condition. The theoretical results, that we review in the following, were established for Ω with a smooth curved (non-polygonal) boundary and finite element approximations were considered for polyhedral domains approximating this smooth domain. These theoretical results differ primarily in the treatment of the boundary flux condition (3).

In one of the simplest formulation, the boundary flux condition (3) is imposed strongly: the velocity approximation is sought in an ansatz space where all vectors satisfy (3) at each nodes when Lagrange finite elements are used. The first convergence results were proved by Verfürth [31]. The convergence rates obtained in [31] are not optimal and were improved by Knobloch [22] and Bänsch and Deckelnick [4], from 1/2 to 3/2 in usual norms, in the case of Taylor–Hood (P_2/P_1) elements. This rate cannot be improved further in general due to the error in the approximation of Ω by polygonal domains Ω_h (see for instance Strang and Fix [29, Section 4.4]).

Interestingly, and in direct relation to our present work, in [31] Verfürth argued that the obtained suboptimal rate could be difficult to improve due to Babuska's like paradox [2,3]. Babuska's paradox can be stated as follows: *the solution of Kirchhoff plate equations with simple support boundary conditions in a disk is not the limit of the solutions to the same equations posed on polygonal domains approaching the disk*, as in Fig. 1 (left). One can then easily imagine that some difficulties may appear when performing finite element approximations of these equations in meshed polygonal domains approaching the disk, like in Fig. 1 (right). This paradox holds in fact whenever a smooth curved boundary is involved (see [23]). That Babuska's like paradox is into play in the case of Stokes equations with slip boundary conditions was pointed out by Verfürth [31] by observing that the stream function formulation of Stokes equations with *free* slip boundary conditions, obtained by posing $\boldsymbol{u} = \mathbf{curl}\,\psi$ (which is possible since $\nabla \cdot \boldsymbol{u} = 0$, and then ψ is the so-called *stream function*), leads to the Kirchhoff plate equation $-\mu\Delta^2\psi = \operatorname{curl} \boldsymbol{f}$ with simple support boundary conditions: $\psi = 0$ and $\Delta\psi = 2\kappa\,\partial\psi/\partial\boldsymbol{\nu}$ (where κ is the curvature of $\partial\Omega$, see for instance [12] for details).

Motivated by the lack of optimality in his estimates, Verfürth [32] proposed to handle the constraint Eq. (3) in a weak way, by the Lagrange multiplier method. With the introduction of a new variable – the Lagrange multiplier-finite element approximation spaces need to be chosen with care (enriching the velocity approximation space with bubble functions having their support in the vicinity of Γ, like in [32], for instance) or residual boundary terms may be added in the original variational formulation of the equations, resulting in a so-called *stabilized* formulation [33]. As Stenberg [28] already observed, formal elimination of the Lagrange multiplier in these stabilized formulations results in problem formulations similar to Nitsche's method [26] to weakly append Dirichlet type boundary conditions.

The objective of this work is to study the efficiency of these two methods (the Lagrange multiplier method and Nitsche's method) to impose in a weak way a slip boundary condition (more precisely flux boundary condition (3)) for Stokes (and Navier–Stokes) equations, and to put into evidence some convergence problems which may be related to Babuska's like paradox, in the case of a domain with a smooth curved boundary. As convergence of finite element approximations are difficult to establish in the case of a smooth curved boundary, and as convergence of these methods depends on the values of some parameters (see Sections 2 and 4) even in the case of a polygonal boundary, we first study these methods theoretically only in the case of a polygonal (or polyhedral) boundary. Then we test them numerically, first with a polygonal boundary (in order to illustrate the theoretical results) and then with a smooth boundary in order to put into evidence the paradox.

In Section 2, after recalling the Lagrange multiplier method, we first describe a set of variants of the stabilized formulation introduced and studied in [33]. In Section 3, we prove the convergence of the resulting approximation method when Ω has a polygonal or polyhedral boundary. The theoretical convergence results depend on the values of the parameters. In Section 4, we prove the stability of several variants of Nitsche's method, depending on the values of the parameters, assuming again that the domain is polygonal (or polyhedral). One of these variants has the advantage of being stable, regardless of the (polygonal) domain, hence its interest for series of polygonal approximations of a smooth domain. Finally, in Section 5, the two classes of approximation methods studied here theoretically for polygonal domains are tested numerically for both polygonal and smooth boundaries. In the case of a 2D polygonal domain, all the tests confirm the theory. But in the case of a domain with a smooth curved boundary (a ring), numerical approximations may not converge towards the exact solution at all, putting into evidence that Babuska's like paradox may be at play. In particular, our numerical results seem to contradict the theoretical convergence results of Verfürth in [33] for the stabilized Lagrange multiplier method. Moreover, we show that this instability with respect to polyhedral perturbations of the domain also appears when using Nitsche's methods studied in Section 4. We draw more precise conclusions in Section 6. Finally, details of the theoretical demonstrations are given in Appendix A.

2. The Lagrange multiplier method

In the remaining of this paper, if ω is a domain of $\mathbf{R}^n$ with boundary γ then $H^k(\omega)$ and $H^{k-1/2}(\gamma)$, $k \geqslant 0$, designate the usual Sobolev spaces. Their usual norms are denoted by $\|.\|_k$ and $\|.\|_{k-1/2,\gamma}$ respectively. Recall that $H^0(\omega) = L^2(\omega)$ and $H^{-1/2}(\gamma)$ is the dual space of $H^{1/2}(\gamma)$. The duality product between $\rho \in H^{-1/2}(\gamma)$ and $\lambda \in H^{1/2}(\gamma)$ is simply denoted by $\langle \rho, \lambda\rangle_\gamma$. Since there cannot be any confusion, the same notations are used for the norms and duality products associated to spaces in product form like $(H^k(\omega))^n$ or $(H^{k-1/2}(\gamma))^n$.

We further adopt the simplifying notation:

$$Q := L_0^2(\Omega) = \left\{ \boldsymbol{v} \in L^2(\Omega)\colon \int\limits_\Omega v\, d\Omega = 0 \right\}, \qquad \Lambda := H^{-1/2}(\Gamma),$$

and we define the quotient space

$$V := H^1(\Omega)/\mathcal{R},$$

where $\mathcal{R}$ is the space of rigid body motions, $\mathcal{R} := \{\boldsymbol{a} + \boldsymbol{b}x\colon \boldsymbol{a} \in \mathbf{R}^n \text{ and } \boldsymbol{b} \in S_n\}$, and S_n is the space of anti-symmetric $n \times n$ matrices. Note that, assuming that Ω has a Lipschitz boundary, functions in V satisfy the second Korn inequality (see [1])

$$\|\boldsymbol{u}\|_{1,\Omega} \leqslant C \left\| D(\boldsymbol{u}) \right\|_{0,\Omega}, \quad \forall \boldsymbol{v} \in V, \tag{5}$$

for some $C > 0$.

A solution of (1)–(4) can be sought as the solution of the saddle-point problem: Find $\boldsymbol{u} \in V$, $p \in Q$ and $\rho \in \Lambda$ such that

$$\mathcal{L}(\boldsymbol{u}, p, \rho) = \inf_{q \in Q,\, \lambda \in \Lambda} \sup_{\boldsymbol{v} \in V} \mathcal{L}(\boldsymbol{v}, q, \lambda),$$

where $\mathcal{L}$ is the Lagrangian functional defined by

$$\mathcal{L}(\boldsymbol{v}, q, \lambda) = \mu \int\limits_\Omega \left|\boldsymbol{D}(\boldsymbol{v})\right|^2 d\Omega - \int\limits_\Omega \boldsymbol{f} \cdot \boldsymbol{v}\, d\Omega - \int\limits_\Omega q \nabla \cdot \boldsymbol{v}\, d\Omega + \int\limits_\Gamma (\boldsymbol{v} \cdot \boldsymbol{\nu} - g)\lambda\, d\Gamma - \sum_{i=1}^{n-1} \int\limits_\Gamma f_2 \boldsymbol{v} \cdot \boldsymbol{\tau_i}\, d\Gamma.$$

The Euler–Lagrange equations associated to this saddle-point problem give the variational formulation: Find $\boldsymbol{u} \in V$, $p \in Q$ and $\rho \in \Lambda$ such that

$$2\mu \int\limits_\Omega \boldsymbol{D}(\boldsymbol{u}) : \boldsymbol{D}(\boldsymbol{v})\, d\Omega - \int\limits_\Omega p\, \nabla \cdot \boldsymbol{v}\, d\Omega + \int\limits_\Gamma \rho\, \boldsymbol{v} \cdot \boldsymbol{\nu}\, d\Gamma = \int\limits_\Omega \boldsymbol{f} \cdot \boldsymbol{v}\, d\Omega + \sum_{i=1}^{n-1} \int\limits_\Gamma f_2\, \boldsymbol{v} \cdot \boldsymbol{\tau_i}\, d\Gamma, \quad \forall \boldsymbol{v} \in V, \tag{6}$$

$$\int\limits_\Omega \nabla \cdot \boldsymbol{u} q\, d\Omega = 0, \quad \forall q \in Q, \tag{7}$$

$$\int\limits_\Gamma \boldsymbol{u} \cdot \boldsymbol{\nu} \lambda\, d\Gamma = \int\limits_\Gamma g \lambda\, d\Gamma, \quad \forall \lambda \in \Lambda. \tag{8}$$

Verfürth [32] proved that this saddle point problem admits a unique solution $(\boldsymbol{u}, p, \rho) \in V \times Q \times \Lambda$ for sufficiently smooth data f, g and $f_{2,i}$, under the assumption that Γ is C^3. His result can nevertheless be extended to domains verifying the elliptic regularity property used in his proof of Lemma 3.1 in [32]:

(H0): $\|\phi\|_{2,\Omega} \leqslant C(\|\psi\|_{0,\Omega} + \|\rho\|_{1/2,\Gamma})$ for any $\psi \in L^2(\Omega)$, $\rho \in H^{1/2}(\Gamma)$, where ϕ is the weak solution of $-\Delta\phi = \psi$ in Ω, $\frac{\partial\phi}{\partial\boldsymbol{\nu}} = \rho$ on Γ.

Remark 2.1. (H0) is satisfied when, for instance, Ω is a bounded convex domain or is a plane bounded domain with Lipschitz and piecewise C^2 boundary whose angles are convex (see Theorem 3.2.1.3 and Remark 3.2.1.4 in [18]).

Of course, (6)–(8) can be obtained from (1)–(4) by suitable multiplications by test functions and integrations by parts and we easily verify that their respective solutions coïncide. Moreover, ρ is the negative of the normal component of the stress tensor:

$$\rho = -\sigma(\boldsymbol{u}, p),$$

where $\sigma(\boldsymbol{u}, p) := \boldsymbol{\nu} \cdot \boldsymbol{T}(\boldsymbol{u}, p) \cdot \boldsymbol{\nu} = -p + 2\mu\boldsymbol{\nu} \cdot \boldsymbol{D}(\boldsymbol{u}) \cdot \boldsymbol{\nu}$.

Let us consider classes of approximation spaces V_h, Q_h and Λ_h for V, Q and Λ respectively. Here, $h > 0$ is a discretization parameter which goes to 0. As we allow Ω to be arbitrarily smooth (and not only a polygon or a polyhedron) we assume that these approximation spaces correspond to polygonal ($n = 2$) or polyhedral ($n = 3$) domains Ω_h approximating Ω as h tends to 0. The boundary of Ω_h is denoted by Γ_h. If Ω is not polyhedral then we assume that each vertex of Ω_h lies in Γ and we define $g_h = I_h g - \int_{\Gamma_h} I_h g\, d\Gamma / \int_{\Gamma_h} d\Gamma$, $f_{2,i,h} = I_h f_{2,i}$, for $i = 1, \dots, n-1$, where $I_h g$ is the continuous piecewise linear function interpolating g at the vertex of Ω_h. If Ω is polyhedral then we assume that $\Omega_h = \Omega$ and we set $g_h = g$ and $f_{2,i,h} = f_{2,i}$. We assume that g and $f_{2,i}$, $i = 1, \dots, n-1$, are functions sufficiently smooth to define these interpolations.

The approximated problem then writes

$$2\mu \int_{\Omega_h} \boldsymbol{D}(\boldsymbol{u}) : \boldsymbol{D}(\boldsymbol{v})\, d\Omega - \int_{\Omega_h} p\, \nabla \cdot \boldsymbol{v}\, d\Omega + \int_{\Gamma_h} \rho\, \boldsymbol{v} \cdot \boldsymbol{\nu}\, d\Gamma = \int_{\Omega_h} \boldsymbol{f} \cdot \boldsymbol{v}\, d\Omega + \sum_{i=1}^{n-1} \int_{\Gamma_h} f_{2,i,h}\, \boldsymbol{v} \cdot \boldsymbol{\tau_i}\, d\Gamma, \quad \forall \boldsymbol{v} \in V_h, \tag{9}$$

$$\int_{\Omega_h} \nabla \cdot \boldsymbol{u} q\, d\Omega = 0, \quad \forall q \in Q_h, \tag{10}$$

$$\int_{\Gamma_h} \boldsymbol{u} \cdot \boldsymbol{\nu} \lambda\, d\Gamma = \int_{\Gamma_h} g_h \lambda\, d\Gamma, \quad \forall \lambda \in \Lambda_h. \tag{11}$$

For the solutions to be uniquely defined and to converge as $h \to 0$ to the solutions of the continuous problem (6)–(8), approximation spaces need to satisfy the inf-sup condition [8]

$$\inf_{q \in Q_h,\, \rho \in \Lambda_h} \sup_{\boldsymbol{v} \in V_h} \frac{-\int_{\Omega_h} q \nabla \cdot \boldsymbol{v}\, d\Omega + \int_{\Gamma_h} \rho \boldsymbol{v} \cdot \boldsymbol{\nu}\, d\Gamma}{(\|q\|_{0,\Omega_h}^2 + \|\rho\|_{-1/2,\Gamma_h}^2)^{1/2} \|\boldsymbol{v}\|_{1,\Omega_h}} > \beta > 0. \tag{12}$$

As demonstrated by Verfürth [32], simple choices for Λ_h combined with classical finite element spaces $V_h \times Q_h$ which satisfy the classical LBB inf-sup condition

$$\inf_{q \in Q_h} \sup_{\boldsymbol{v} \in V_h} \frac{\int_{\Omega_h} q \nabla \cdot \boldsymbol{v}\, d\Omega}{\|q\|_{0,\Omega_h} \|\boldsymbol{v}\|_{1,\Omega_h}} > \beta > 0 \tag{13}$$

may fail to satisfy (12).

A way to obtain a stable approximation is to enrich V_h with suitable bubble functions having support in the elements that are along Γ_h. Before introducing these functions, let us first introduce our notation and our assumptions about the meshes.

For any $h > 0$, let $\mathcal{T}_h$ be a triangulation of Ω_h in *n-simplices* having a diameter smaller than h and such that any intersection of two simplices is either empty, a vertex, an edge or a face. We assume that the partitioning is regular, in the sense that there exists $C > 0$ such that for every element $T \in \mathcal{T}_h$, its diameter h_T and the diameter d_T of the largest ball contained in T verify $h_T < C d_T$. The resulting partitioning of Γ_h into segments or triangles is denoted by $\mathcal{S}_h$. The diameter of a given element $S \in \mathcal{S}_h$ is denoted by h_S.

Let $S \in \mathcal{S}_h$ and denote by T_S the element of $\mathcal{T}_h$ of which S is a face or an edge. Denote by $\lambda_{T_S,1}, \dots, \lambda_{T_S,n+1}$ the barycentric coordinates of T_S, the last one being associated with the vertex of T_S which does not lie on $\bar{S}$, and define

$$\boldsymbol{\phi}_S := \begin{cases} \prod_{i=1}^n \lambda_{T_S,i} \boldsymbol{\nu}_h & \text{on } T_S, \\ 0 & \text{elsewhere.} \end{cases} \tag{14}$$

The space of bubble functions is defined by

$$B_h := \bigcup_{S \in \mathcal{S}_h} B_{S,h}, \quad \text{with } B_{S,h} := \{ r\boldsymbol{\phi}_S \colon r \in P_m(T_S) \}, \tag{15}$$

where $P_m(T)$ is the space of polynomials of degree m or less. Let us denote by N_S the dimension of $P_m(T)$. If for instance $m = 0$ then $N_S = 1$. Let $\{b_{S,1}, \dots, b_{S,N_S}\}$ denote a basis of $B_{S,h}$. We define $\tilde{V}_h = V_h + B_h$. An element $\tilde{\boldsymbol{u}} \in \tilde{V}_h$ can then be written

$$\tilde{\boldsymbol{u}} = \boldsymbol{u} + \sum_{S \in \mathcal{S}_h} \sum_{1 \leqslant i \leqslant N_S} \alpha_{S,i} b_{S,i}, \quad \alpha_{S,i} \in \mathbf{R}$$

with $\boldsymbol{u} \in V$. The *bubble-stabilized* formulation is then (9)–(11) with V_h replaced by $\tilde{V}_h$. Here V_h and Q_h are assumed to be popular finite element spaces for Stokes equations with Dirichlet boundary conditions, in particular satisfying (13), whereas Λ_h is the space of piecewise polynomials of degree m or less on each element of $\mathcal{S}_h$. These spaces will be specified and used later in this work. We also refer to Verfürth [32] for more details about the approximation spaces and for convergence results about this method.

3. Stabilized formulations

A way to circumvent the inf-sup condition (12) for finite elements already satisfying (13) is to add suitable residual terms in the weak equations (6)–(8), resulting in a *stabilized* formulation. These stabilization procedures were originally developed in order to circumvent the classical LBB inf-sup condition (13) (see for instance Hughes et al. [21]). Here, we assume that V_h and Q_h satisfy (13) and the objective is to circumvent (12).

Let us introduce the bilinear and linear forms defined by

$$a_h(\boldsymbol{u}, \boldsymbol{v}) = 2\mu \int_{\Omega_h} \boldsymbol{D}(\boldsymbol{u}) : \boldsymbol{D}(\boldsymbol{v})\, d\Omega, \qquad \ell_{\Omega_h}(\boldsymbol{v}) = \int_{\Omega_h} \boldsymbol{f} \cdot \boldsymbol{v}\, d\Omega,$$

$$b_{\Omega_h}(\boldsymbol{u}, p) = -\int_{\Omega_h} p\, \nabla \cdot \boldsymbol{v}\, d\Omega, \qquad b_{\Gamma_h}(\rho, \boldsymbol{u}) = \int_{\Gamma_h} \rho\, \boldsymbol{u} \cdot \boldsymbol{v}\, d\Gamma,$$

$$\ell_{\Gamma_h,1}(\rho) = \int_{\Gamma_h} g_h \rho\, d\Gamma, \qquad \ell_{\Gamma_h,2}(\boldsymbol{v}) = \sum_{i=1}^{n-1} \int_{\Gamma_h} f_{2,i,h}\, \boldsymbol{v} \cdot \boldsymbol{\tau_i}\, d\Gamma,$$

which we use to define the bilinear form $\mathcal{B}_h$ and the linear form $\mathcal{L}_h$ by

$$\mathcal{B}_h\big((\boldsymbol{u}, p, \rho), (\boldsymbol{v}, q, \lambda)\big) = a_h(\boldsymbol{u}, \boldsymbol{v}) + b_{\Omega_h}(\boldsymbol{v}, p) + b_{\Gamma_h}(\rho, \boldsymbol{v}) + \gamma b_{\Omega_h}(\boldsymbol{u}, q) + b_{\Gamma_h}(\lambda, \boldsymbol{u}),$$
$$\mathcal{L}_h(\boldsymbol{v}, q, \lambda) = \ell_{\Omega_h}(\boldsymbol{v}) + \ell_{\Gamma_h,2}(\boldsymbol{v}) + \ell_{\Gamma_h,1}(\lambda),$$

where γ is a constant parameter with value 1 or -1.

The approximation problem (9)–(11) then writes: Find $\boldsymbol{u}_h \in V_h$, $p_h \in Q_h$ and $\rho_h \in \Lambda_h$ such that

$$\mathcal{B}_h\big((\boldsymbol{u}_h, p_h, \rho_h), (\boldsymbol{v}, q, \lambda)\big) = \mathcal{L}_h(\boldsymbol{v}, q, \lambda), \quad \forall(\boldsymbol{v}, q, \lambda) \in V_h \times Q_h \times \Lambda_h. \tag{16}$$

Note that, although $\mathcal{B}_h$ is symmetric only when $\gamma = 1$, the two Eqs. (16) corresponding to the two admissible values for γ are equivalent. One can be deduced from the other by the change of variable $q \to -q$.

In order to introduce the stabilized formulations let us define the mesh-dependent bilinear form

$$\langle \rho, \lambda \rangle_{-\frac{1}{2},h,\Gamma_h} = \sum_{S \in \mathcal{S}_h} h_S \int_S \rho\lambda\, d\Gamma, \quad \forall \rho, \lambda \in \Lambda_h \tag{17}$$

as well as the associated *discrete* norm $\|.\|_{-\frac{1}{2},h,\Gamma_h}$ defined by

$$\|\rho\|_{-\frac{1}{2},h,\Gamma_h} = \langle \rho, \rho \rangle^{1/2}_{-\frac{1}{2},h,\Gamma_h}.$$

Define the bilinear form

$$\mathcal{B}_{\alpha,h}\big((\boldsymbol{u}, p, \rho), (\boldsymbol{v}, q, \lambda)\big) = \mathcal{B}_h\big((\boldsymbol{u}, p, \rho), (\boldsymbol{v}, q, \lambda)\big) - \alpha\big\langle \rho + \sigma(\boldsymbol{u}, p), \lambda + \delta\sigma(\boldsymbol{v}, q)\big\rangle_{-\frac{1}{2},h,\Gamma_h},$$

where α and δ are real parameters that are discussed in what follows. The stabilized formulation that we shall study then writes: Find $\boldsymbol{u} \in V_h$, $p \in Q_h$ and $\rho \in \Lambda_h$ such that

$$\mathcal{B}_{\alpha,h}\big((\boldsymbol{u}, p, \rho), (\boldsymbol{v}, q, \lambda)\big) = \mathcal{L}_h(\boldsymbol{v}, q, \lambda), \quad \forall(\boldsymbol{v}, q, \lambda) \in V_h \times Q_h \times \Lambda_h. \tag{18}$$

Note that when Ω has a polygonal or polyhedral boundary (and then $\Omega_h = \Omega$), if the approximation is conformal (that is if $V_h \subset V$, $Q_h \subset Q$ and $\Lambda_h \subset \Lambda$) then the approximation method is consistent in the sense that a smooth solution $(\boldsymbol{u}, p, \rho) \in V \times Q \times \Lambda$ of the continuous problem also satisfies (18).

Note also that, although not explicit in the notation, $\mathcal{B}_{\alpha,h}$ depends on δ and γ. Moreover, contrarily to Eqs. (16), Eqs. (18) corresponding to different parameter values are not generally equivalent one to another.

In this work, we are going to consider the cases where $\alpha > 0$ and $\delta = -1$ or $\delta = 1$.

Verfürth [33] considered the case $\delta = 0$ (with $\gamma = 1$). This normal stress stabilization procedure is inspired from the original pressure stabilization procedure used in [21]. Note that it automatically breaks the symmetry of the original equations (16). Moreover, Verfürth [33] proved that this stabilized formulation is stable if α is lower than a threshold value which can be difficult to estimate in practice.

If we want the stabilized formulation to remain symmetric then we have to set $\delta = 1$ and $\gamma = 1$. With $\delta = 1$, this can be seen as an adaptation of a stabilization procedure originally devised by Hughes and Franca [20] to circumvent the classical LBB inf-sup condition (13). Its main drawback, at least in [20], is again that $\alpha > 0$ has to be small enough.

In the case $\delta = -1$, this is an adaptation of a stabilized procedure originally devised by Douglas and Wang [14] and later simplified by Franca and Stenberg [16], again to circumvent the classical LBB inf-sup condition (13). The resulting system is no longer symmetric but the stabilized formulations in [14,16] were proved to be *unconditionally stable*, which is to say without restriction on α other than $\alpha > 0$.

In both cases $\delta = 1$ and $\delta = -1$, this stabilization procedure has been applied by Barbosa and Hughes [5] to weakly impose Dirichlet boundary conditions for elliptic equations. They arrived to an analogous conclusion: conditional stability of the method in the case $\delta = 1$ and unconditional stability in the case $\delta = -1$.

Here, for our stabilized formulation (18), we shall only prove the conditional stability of the method for all the aforementioned values of δ and γ. The reason for this limitation is given in Remark 3.2.

Following [33], in order to prove these stability results we make classical assumptions (assumptions (H1)–(H4) in Appendix A) which are verified by classical finite element spaces $V_h \times Q_h$ such as MINI (P_1-bubble/P_1), Taylor–Hood (P_2/P_1) or conformal Crouzeix–Raviart (P_2-bubble/discontinuous P_1) finite element spaces [33].

Let us also introduce the norm $|||\cdot|||_{\alpha,h}$ defined by

$$\left|\left|\left|(\boldsymbol{u}, p, \rho)\right|\right|\right|_h^2 = \left\|D(\boldsymbol{u})\right\|_{0,\Omega_h}^2 + \|p\|_{0,\Omega_h}^2 + \|\rho\|_{-1/2,\Gamma_h}^2 + \|\rho\|_{-\frac{1}{2},h,\Gamma_h}^2,$$

for all $(\boldsymbol{u}, p, \rho) \in V_h \times Q_h \times \Lambda_h$.

Proposition 1. *With $\delta = \pm 1$, $\gamma = \pm 1$ and under assumptions* (H0)–(H4)*, there exists $\alpha_0 > 0$ such that for every $0 < \alpha < \alpha_0$, there exists $C > 0$ such that*

$$\sup_{(\boldsymbol{v},q,\lambda)\in V_h\times Q_h\times\Lambda_h} \frac{\mathcal{B}_{\alpha,h}((\boldsymbol{u}, p, \rho), (\boldsymbol{v}, q, \lambda))}{|||(\boldsymbol{v}, q, \lambda)|||_h} \geqslant C\left|\left|\left|(\boldsymbol{u}, p, \rho)\right|\right|\right|_h,$$

for all $(\boldsymbol{u}, p, \rho) \in V_h \times Q_h \times \Lambda_h$.

Proof. See Appendix A (Section A.1). □

Remark 3.1. Note that even in the case $\delta = -1$ we were not able to prove that the formulation is unconditionally stable. The reason is that, with $\delta = \pm 1$, the smallness condition on α is partly due to condition (28) which enables one to control the last negative term involving the pressure in (27). When $\delta = 0$ (the case studied in [32]), condition (28) does not rule but then the smallness condition is due to (24).

As done in [32], from the stability result we can deduce a convergence result by assuming that the finite element spaces have approximation properties (H5)–(H10) listed in Section A.1. Again, these properties are satisfied by usual finite element spaces like spaces of piecewise polynomials of a given degree, continuous or not, eventually enriched with suitable bubble functions in order to satisfy (H1).

Theorem 1. *With Ω a polygon or a polyhedron, assume* (H0)–(H10) *and assume that the solution $(\boldsymbol{u}, p, \rho)$ of the continuous problem* (6)–(8) *is sufficiently smooth. If α is sufficiently small then the approximate problem* (18) *admits a unique solution $(\boldsymbol{u}_h, p_h, \rho_h)$ which satisfies*

$$\left\|D(\boldsymbol{u} - \boldsymbol{u}_h)\right\|_{0,\Omega} + \|p - p_h\|_{0,\Omega} + \|\rho - \rho_h\|_{-1/2,\Gamma} + h^{1/2}\|\rho - \rho_h\|_{0,\Gamma} \leqslant h^s\left(\|\boldsymbol{f}\|_{0,\Omega} + \|g\|_{3/2,\Gamma} + \|f_{2,i}\|_{1/2,\Gamma}\right). \tag{19}$$

Remark 3.2. Verfürth [32] gives a proof for $\delta = 0$ and when Ω has a $\mathcal{C}^3$ boundary. The result is a direct consequence of the stability property of Proposition 1 and of approximation properties (H5)–(H10). As the approximation method is consistent when Ω is polygonal or polyhedral, there is no consistency error to estimate and the proof is easier. Although the polygonal or polyhedral case is not a particular case of the $\mathcal{C}^3$ case, the proof of Theorem 1 is easier, can be extracted from the proof of Proposition 4.2 in [32] and is not repeated here.

Remark 3.3. From Korn inequality (5), it follows that the error estimate on the velocity contained in (19) is equivalent to an error estimate in the space $V = H^1(\Omega)/\mathcal{R}$.

Example 3.1.

- If we take piecewise constant functions (P_0) for Λ_h together with MINI (P_1-bubble/P_1, see [8]) finite element space for $V_h \times Q_h$, then (19) holds with $s = 1$.
- For the convergence to be quadratic ($s = 2$), we can take for instance the P_1^{disc} finite element for Λ_h, combined with Taylor–Hood (P_2/P_1) finite elements for $V_h \times Q_h$. If Taylor–Hood finite elements are combined with P_0 instead, we obtain a linear convergence only.

4. Nitsche's method

Stenberg [28] noticed that, in the case of a scalar elliptic equation, one of the stabilized formulations studied by Barbosa and Hughes [5] to append a Dirichlet boundary condition using the Lagrange multiplier method is connected to Nitsche's method [26]. Nitsche's method was originally devised for elliptic equations to append the Dirichlet boundary condition in a weak way but the method does not rely on a Lagrange multiplier. The connection between the two methods was established in [28] by simply eliminating the Lagrange multiplier, resulting in a close variant of Nitsche's method.

Let us conduct a similar operation for our problem. Let us first assume that $\Omega_h = \Omega$ for every $h > 0$. This is to say we assume that Ω is polygonal or polyhedral. Now, set $v = 0$ and $q = 0$ in (18). We then obtain

$$\int_{\Gamma_h} \lambda \boldsymbol{u}\cdot\boldsymbol{\nu}\,d\Gamma - \alpha\big\langle \rho + \sigma(\boldsymbol{u}, p), \lambda\big\rangle_{-\frac{1}{2},h,\Gamma_h} = \int_{\Gamma_h} g_h \lambda\,d\Gamma, \quad \forall\lambda \in \Lambda_h,$$

from which it follows that

$$\int_S \rho\lambda\,d\Gamma = \int_S \left(-\sigma(\boldsymbol{u}, p) + \frac{\boldsymbol{u}\cdot\boldsymbol{\nu} - g_h}{\alpha h_S}\right)\lambda\,d\Gamma, \quad \forall S \in \mathcal{S}_h,\ \forall\lambda \in \Lambda_h.$$

Observe that ρ can be identified as the $L^2(\Gamma_h)$ projection onto Λ_h of the function whose restriction to each $S \in \mathcal{S}_h$ is $-\sigma(\boldsymbol{u}, p) + \frac{\boldsymbol{u}\cdot\boldsymbol{\nu}-g_h}{\alpha h_S}$. Although the following property is obviously not true, let us assume that we exactly have $\rho_{|S} = -\sigma(\boldsymbol{u}, p) + \frac{\boldsymbol{u}\cdot\boldsymbol{\nu}-g_h}{\alpha h_S}$ (recall that in the continuous case $\boldsymbol{u}\cdot\boldsymbol{\nu} = g$ and $\rho = -\sigma(\boldsymbol{u}, p)$). Substituting ρ and taking $\lambda = 0$ reduces (18) to

$$\mathcal{D}_{\alpha,h}\big((\boldsymbol{u}, p), (\boldsymbol{v}, q)\big) = \mathcal{F}_\delta(\boldsymbol{v}, q), \quad \forall(\boldsymbol{v}, q) \in V_h \times Q_h, \tag{20}$$

where

$$\mathcal{D}_{\alpha,h}\big((\boldsymbol{u}, p), (\boldsymbol{v}, q)\big) = a_h(\boldsymbol{u}, \boldsymbol{v}) + b_{\Omega_h}(\boldsymbol{v}, p) + \gamma b_{\Omega_h}(\boldsymbol{u}, q) - b_{\Gamma_h}\big(\sigma(\boldsymbol{u}, p), \boldsymbol{v}\big) - \delta b_{\Gamma_h}\big(\sigma(\boldsymbol{v}, q), \boldsymbol{u}\big) + \frac{1}{\alpha}\langle \boldsymbol{u}\cdot\boldsymbol{\nu}, \boldsymbol{v}\cdot\boldsymbol{\nu}\rangle_{\frac{1}{2},h,\Gamma_h},$$

and

$$\mathcal{F}_{\delta,h}(\boldsymbol{v}, q) = \ell_{\Omega_h}(\boldsymbol{v}) + \ell_{\Gamma_h,2}(\boldsymbol{v}) - \delta\,\ell_{\Gamma_h,1}\big(\boldsymbol{\nu}\cdot T(\boldsymbol{v}, q)\big) + \frac{1}{\alpha}\langle g_h, \boldsymbol{v}\cdot\boldsymbol{\nu}\rangle_{\frac{1}{2},h,\Gamma_h}.$$

Here, we have used the discrete scalar product $\langle\cdot,\cdot\rangle_{\frac{1}{2},h,\Gamma}$ defined by

$$\langle \rho, \lambda\rangle_{\frac{1}{2},h,\Gamma_h} = \sum_{S\in\mathcal{S}_h} \frac{1}{h_S}\int_S \rho\lambda\,d\Gamma$$

and with associated norm $\|\rho\|_{\frac{1}{2},h,\Gamma} = \langle \rho, \rho\rangle^{1/2}_{\frac{1}{2},h,\Gamma}$.

Formulation (20) can be obtained directly from Eqs. (1)–(4). Moreover, in the case where Ω is polygonal or polyhedral, the solution $(\boldsymbol{u}, p)$ of (1)–(4) satisfies $\mathcal{D}_{\alpha,h}((\boldsymbol{u}, p), (\boldsymbol{v}, q)) = \mathcal{F}_\delta(\boldsymbol{v}, q)$ for all $(\boldsymbol{v}, q) \in V \times Q$. Since $V_h \subset V$ and $Q_h \subset Q$ in this case, the consistency property of the approximation method (20) follows:

Lemma 1. *Assume that Ω has a polygonal or polyhedral boundary. Let $(\boldsymbol{u}, p)$ and $(\boldsymbol{u}_h, p_h)$ be the solutions of (1)–(4) and (20) respectively. They satisfy*

$$\mathcal{D}_{\alpha,h}\big((\boldsymbol{u}, p) - (\boldsymbol{u}_h, p_h), (\boldsymbol{v}_h, q_h)\big) = 0, \quad \forall(\boldsymbol{v}, q) \in V_h \times Q_h. \tag{21}$$

With $\delta = 0$, regardless of the choice for γ, (20) is the original Nitsche's method [26] which was applied to elliptic equations with a Dirichlet boundary condition. However, the most commonly used variant consists in taking $\delta = 1$ (see for instance Fairweather [15]). In the latter case, when the original system is symmetric, like here Stokes equations with $\gamma = 1$, the resulting system remains symmetric. Hansbo and Larson [19] as well as Burman and Hansbo [9] proved the stability of two *discontinuous* Galerkin formulations of (20) with additional stabilizing terms involving inter-element edge jumps (and with $\delta = 1$).

Here we shall prove the stability of (20) for sufficiently small α, regardless of the choice for δ and γ, like for stabilized formulations. Moreover, we shall prove that with $\delta = -1$ and $\gamma = -1$, Nitsche's method (20) is unconditionally stable, this is to say without any condition on α besides $\alpha > 0$. This result is in contrast with the conditional stability result of the stabilized Lagrange multiplier method obtained in the previous section even with $\delta = -1$ and $\gamma = -1$. A similar unconditional stability result for this non-symmetric variant of Nitsche's method was already proved for scalar elliptic equations with a Dirichlet boundary condition in [17].

For the following stability result we need to introduce the norm $\|.\|_h$ defined by

$$\left\|(\boldsymbol{u}, p)\right\|_h^2 = \left\|D(\boldsymbol{u})\right\|_{0,\Omega}^2 + \|p\|_{0,\Omega}^2 + \frac{1}{\alpha}\|\boldsymbol{u}\cdot\boldsymbol{\nu}\|_{\frac{1}{2},h,\Gamma}^2.$$

Proposition 2. *Let us assume that* (H1)–(H3) *hold.*

(i) *If* $\delta = \pm 1$ *and* $\gamma = \pm 1$ *then there exists* $\alpha_0 > 0$ *such that: for all* $0 < \alpha < \alpha_0$ *there exists* $C > 0$ *independent of* h *such that*

$$\sup_{(\boldsymbol{v},q)\in V_h\times Q_h} \frac{\mathcal{D}_{\alpha,h}((\boldsymbol{u},p),(\boldsymbol{v},q))}{\|(\boldsymbol{v},q)\|_h} \geqslant C\left\|(\boldsymbol{u},p)\right\|_h, \quad \forall(\boldsymbol{u},p)\in V_h\times Q_h. \tag{22}$$

(ii) *If* $\delta = -1$ *and* $\gamma = -1$ *then* (22) *is valid for all* $\alpha > 0$.

Proof. See Appendix A (Section A.2). □

We are now in position to prove the following convergence result when Ω is a polygon or a polyhedron.

Theorem 2. *Assume* (H0)–(H2), (H4)–(H7) *and assume that* Ω *has a polygonal or polyhedral boundary. We also assume that the conditions on* α *provided by Proposition 2 to ensure uniform stability are met. Let* $(\boldsymbol{u}, p)$ *and* $(\boldsymbol{u}_h, p_h)$ *be the solutions of* (1)–(4) *and* (20) *respectively. If* $(\boldsymbol{u}, p)$ *is sufficiently smooth then they satisfy*

$$\left\|(\boldsymbol{u},p)-(\boldsymbol{u}_h,p_h)\right\|_h \leqslant h^s\left(\|\boldsymbol{u}\|_{s+1,\Omega_h} + \|p\|_{s,\Omega_h}\right). \tag{23}$$

Proof. See Appendix A (Section A.3). □

Example 4.1.

- If we take MINI (P_1-bubble/P_1) finite element space for $V_h \times Q_h$, then (23) holds with $s = 1$.
- For the convergence to be quadratic ($s = 2$), we can take for instance Taylor–Hood (P_2/P_1) finite elements.

5. Numerical examples

In this section numerical results in dimension $n = 2$ are compared to the theoretical convergence results provided in Sections 3 and 4 for the stabilized formulation of the Lagrange multiplier method (18) and for Nitsche's method (20) respectively. We consider two types of domains. In the first example Ω has a polygonal geometry (a square) so that the assumptions of the above mentioned theoretical convergence results are met. In the second example (a ring), Ω has a smooth boundary. This enable us to put in evidence convergence difficulties, depending on the formulations, on the values of some of the parameters and on the finite elements used.

To observe these convergence properties we shall use the technique of manufactured solutions. An analytical divergence-free velocity field and a pressure field are substituted in the Stokes equations to yield balancing volumetric forces terms. These terms are used throughout a standard mesh refinement study.

Since our goal is to put in evidence convergence problems principally for the velocity approximation, the manufactured pressure solution is $p = 0$ in all the tests presented here.

5.1. A simple polygonal geometry

In this example, Ω is the square $\{(x, y),\ -1 < x < 1,\ -1 < y < 1\}$. Throughout the analysis, polygonal domains Ω_h remain identical to Ω, while meshes are generated in a structured manner and made of $2 \times N \times N$ square triangles of side length $h = 1/N$.

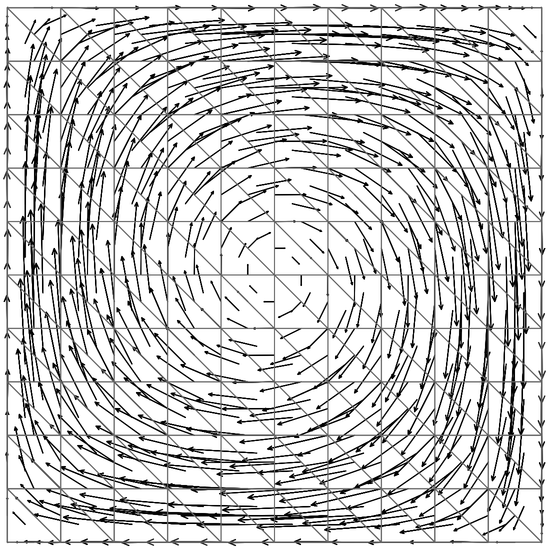

Fig. 2. The $2 \times 10 \times 10$ triangles structured mesh and a finite element approximation of velocity field $\boldsymbol{u} = (2y(1-x^2), -2x(1-y^2))$ using stabilized Lagrange multiplier method (18).

Table 1
Stabilized Lagrange multiplier method (18) in the square. Parameters values are $\mu = 1$, $\alpha = 4$, $\gamma = 1$, $\delta = -1$, and the exact solution is $\boldsymbol{u} = (2y(1-x^2), -2x(1-y^2))$, $p = 0$.

h	MINI-P_0		TH-P_1	
	$\Vert\boldsymbol{u}_h - \boldsymbol{u}\Vert_{1,\Omega}$	$\Vert p_h - p\Vert_{0,\Omega}$	$\Vert\boldsymbol{u}_h - \boldsymbol{u}\Vert_{1,\Omega}$	$\Vert p_h - p\Vert_{0,\Omega}$
1/10	1.55	7.91×10^{-4}	6.84×10^{-2}	8.21×10^{-7}
1/20	7.68×10^{-1}	3.08×10^{-4}	1.74×10^{-2}	1.05×10^{-7}
1/40	3.80×10^{-1}	1.12×10^{-4}	4.38×10^{-3}	1.32×10^{-8}
1/80	1.88×10^{-1}	4.00×10^{-5}	1.10×10^{-3}	1.66×10^{-9}
Rate	1.0	1.5	2.0	3.0

Table 2
Nitsche's method (20) in the square. Parameters values are $\mu = 1$, $\alpha = 4$, $\gamma = 1$, $\delta = -1$, and the exact solution is $\boldsymbol{u} = (2y(1-x^2), -2x(1-y^2))$, $p = 0$.

h	MINI		TH	
	$\Vert\boldsymbol{u}_h - \boldsymbol{u}\Vert_{1,\Omega}$	$\Vert p_h - p\Vert_{0,\Omega}$	$\Vert\boldsymbol{u}_h - \boldsymbol{u}\Vert_{1,\Omega}$	$\Vert p_h - p\Vert_{0,\Omega}$
1/10	2.421	1.99×10^{-3}	7.02×10^{-2}	2.07×10^{-6}
1/20	1.03	7.57×10^{-4}	1.76×10^{-2}	2.61×10^{-7}
1/40	4.54×10^{-1}	2.74×10^{-4}	4.40×10^{-3}	3.27×10^{-8}
1/80	2.08×10^{-1}	9.82×10^{-5}	1.10×10^{-3}	4.10×10^{-9}
Rate	1.0	1.5	2.0	3.0

We first look at the efficiency of the methods in approximating the velocity field $\boldsymbol{u} = (2y(1-x^2), -2x(1-y^2))$ and the pressure $p = 0$, the exact solution of (1)–(4) for suitable data. Note that $\boldsymbol{u}$ is divergence-free, $\nabla \cdot \boldsymbol{u} = 0$, and that $\boldsymbol{u}(x) \cdot \boldsymbol{\nu}(x) = 0$ for all $x \in \Gamma$. Fig. 2 shows the structured mesh corresponding to $h = 1/10$ and the velocity field.

Table 1 shows the approximation errors using the stabilized formulation (18) with MINI-P_0 and TH-P_1 finite elements. Estimated convergence rates confirm the theoretical values predicted in Theorem 1 (see Example 3.1). The convergence rates for the pressure are slightly better than what is predicted, probably due to the structured configuration of the mesh and to the simplicity of the exact pressure solution ($p = 0$).

The same observations can be made for Nitsche's method (20), as shown in Table 2. Convergence rates obtained using MINI and TH finite elements confirm the theoretical results of Theorem 2 (see Example 4.1).

We have repeated this study with a non-polynomial velocity field $\boldsymbol{u} = (-y\sqrt{(x^2+y^2)}, x\sqrt{(x^2+y^2)})$ which again is divergence-free, and with $p = 0$. Note that the boundary flux $\boldsymbol{u} \cdot \boldsymbol{\nu}$ doesn't vanish everywhere on Γ, so that a non-homogeneous boundary flux condition (3) must be imposed. As shown in Tables 3 and 4, theoretical convergence rates are again confirmed, both using the stabilized Lagrange multiplier method and Nitsche's method. On the following subsection, this manufactured solution is tested on another domain Ω, which has a smooth curved boundary.

Table 3
Stabilized Lagrange multiplier method (18) in the square. Parameters values are $\mu = 1$, $\alpha = 4$, $\gamma = 1$, $\delta = -1$, and the exact solution is $\boldsymbol{u} = (-y\sqrt{(x^2+y^2)}, x\sqrt{(x^2+y^2)})$, $p = 0$.

h	MINI-P_0		TH-P_1	
	$\lVert\boldsymbol{u}_h - \boldsymbol{u}\rVert_{1,\Omega}$	$\lVert p_h - p\rVert_{0,\Omega}$	$\lVert\boldsymbol{u}_h - \boldsymbol{u}\rVert_{1,\Omega}$	$\lVert p_h - p\rVert_{0,\Omega}$
1/10	4.86×10^{-1}	1.36×10^{-4}	3.75×10^{-2}	7.77×10^{-7}
1/20	2.45×10^{-1}	5.34×10^{-5}	1.11×10^{-2}	1.56×10^{-7}
1/40	1.22×10^{-1}	1.94×10^{-5}	3.25×10^{-3}	3.47×10^{-8}
1/80	6.11×10^{-2}	6.90×10^{-6}	9.39×10^{-4}	7.73×10^{-9}
Rate	1.0	1.5	1.9	2.2

Table 4
Nitsche's method (20) in the square. Parameters values are $\mu = 1$, $\alpha = 4$, $\gamma = 1$, $\delta = -1$, and the exact solution is $\boldsymbol{u} = (-y\sqrt{(x^2+y^2)}, x\sqrt{(x^2+y^2)})$, $p = 0$.

h	MINI		TH	
	$\lVert\boldsymbol{u}_h - \boldsymbol{u}\rVert_{1,\Omega}$	$\lVert p_h - p\rVert_{0,\Omega}$	$\lVert\boldsymbol{u}_h - \boldsymbol{u}\rVert_{1,\Omega}$	$\lVert p_h - p\rVert_{0,\Omega}$
1/10	6.33×10^{-1}	3.85×10^{-4}	3.33×10^{-2}	7.28×10^{-7}
1/20	2.84×10^{-1}	1.42×10^{-4}	9.45×10^{-3}	9.39×10^{-8}
1/40	1.32×10^{-1}	4.99×10^{-5}	2.61×10^{-3}	1.63×10^{-8}
1/80	6.37×10^{-2}	1.75×10^{-5}	7.09×10^{-4}	3.54×10^{-9}
Rate	1.0	1.5	1.9	2.1

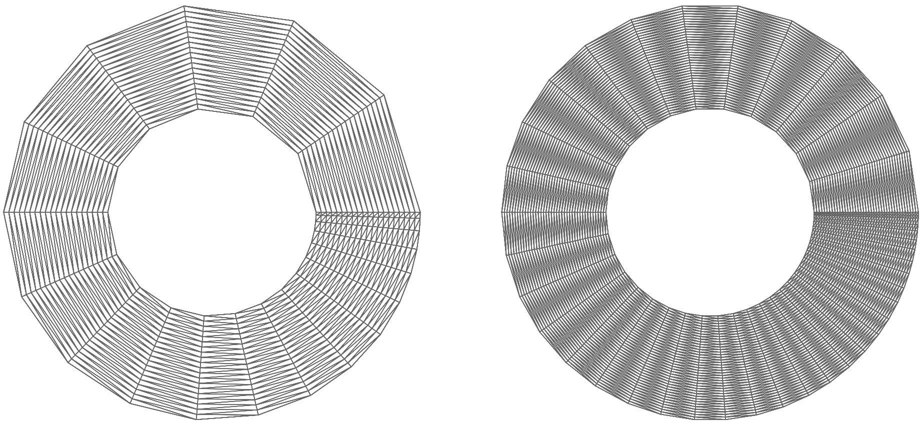

Fig. 3. Left: initial mesh ($h = 1$). Right: first refined mesh ($h = 1/2$).

5.2. A simple non-polygonal geometry

In this example, Ω is the ring $\{(x, y) \in \mathbf{R}^2\colon\ 1 < x^2 + y^2 < 4\}$ and we compute finite element approximations of the manufactured solution

$$\boldsymbol{u} = \left(-y\sqrt{(x^2+y^2)}, x\sqrt{(x^2+y^2)}\right), \quad p = 0.$$

Note that $\nabla \cdot \boldsymbol{u} = 0$ and that $\boldsymbol{u} \cdot \boldsymbol{\nu} = 0$ on Γ. A Dirichlet boundary condition is applied on the inner boundary of the ring, while slip boundary condition (3)–(4) with $g = 0$ and a suitable tangential force f_2 is applied on the outer boundary. All the results shown in what follows were obtained with $\mu = 1$.

Polygonal domains Ω_h and corresponding meshes are built in a structured manner without being regular and homogeneous respectively. The starting mesh is refined several times so as to successively divide by 2 the smaller element side length h. For elements along the boundary, we have been careful to place each boundary vertex of each refined mesh on the original curved boundary Γ. Fig. 3 shows the first two meshes of this series.

5.2.1. Stabilized Lagrange multiplier method

In this section we perform the computations with the stabilized Lagrange multiplier method (18) and observe the convergence rates to the analytical solution. We test several choices of finite elements:

- MINI or Taylor–Hood elements for velocity and pressure.
- P_0 or P_1 (discontinuous) elements for the multiplier.

Table 5
Errors with the stabilized Lagrange multiplier method in the ring, using MINI-P_0 elements, $\gamma = -1$, $\delta = -1$.

α	1	10^{-1}	10^{-2}	10^{-3}	10^{-4}	10^{-5}	10^{-6}
$\|p_h - p\|_0$							
h	9.43669	11.0045	13.5166	16.3318	17.2608	17.3803	17.3926
$h/2$	5.48852	5.75557	6.34192	7.51153	8.33501	8.48879	8.50559
$h/4$	3.45846	3.51335	3.66331	4.03159	4.5201	4.70619	4.73132
$h/8$	2.11496	1.12273	2.14744	2.22128	2.36296	2.4801	2.50698
$h/16$	1.09077	1.09137	1.09331	1.10017	1.11757	1.14282	1.15565
$\|\boldsymbol{u}_h - \boldsymbol{u}\|_1$							
h	2.06405	2.06767	2.07773	2.10445	2.11987	2.12217	2.12241
$h/2$	1.05641	1.05638	1.05752	1.06265	1.06889	1.07033	1.07049
$h/4$	0.530527	0.530516	0.530807	0.531897	0.533584	0.534443	0.534575
$h/8$	0.265115	0.265107	0.261573	0.265423	0.265787	0.266115	0.266216
$h/16$	0.132345	0.132341	0.132353	0.132408	0.132489	0.132566	0.13262

Table 6
Errors with the stabilized Lagrange multiplier method in the ring, using MINI-P_0 elements, $\gamma = 1$, $\delta = -1$.

α	1	10^{-1}	10^{-2}	10^{-3}	10^{-4}	10^{-5}	10^{-6}
$\|p_h - p\|_0$							
h	1315.96	25891.6	397.954	74.4224	6.25436	16.2427	17.2785
$h/2$	1277.66	199.787	610.158	97.8299	4.34182	7.2133	8.37763
$h/4$	1264.55	3058.56	678.897	107.179	8.70953	3.36261	4.5963
$h/8$	1267.27	960.322	696.119	110.301	10.9085	1.12589	2.36999
$h/16$	1263.8	2779.97	695.435	111.186	11.9908	0.259907	1.01879
$\|\boldsymbol{u}_h - \boldsymbol{u}\|_1$							
h	15.2187	296.406	5.60055	2.26021	2.11224	2.12104	2.1223
$h/2$	7.39101	3.23629	3.68055	1.204	1.06875	1.07009	1.07047
$h/4$	3.65983	8.78058	2.02009	0.615154	0.53422	0.534382	0.534567
$h/8$	1.8383	1.8751	1.03489	0.309349	0.266279	0.266102	0.266214
$h/16$	0.919223	2.00648	0.519569	0.154785	0.132779	0.132565	0.132619

Table 7
Errors with the stabilized Lagrange multiplier method in the ring, using MINI-P_0 elements, $\gamma = -1$, $\delta = 0$.

α	1	10^{-1}	10^{-2}	10^{-3}	10^{-4}	10^{-5}	10^{-6}
$\|p_h - p\|_0$							
h	7074.26	2709.92	441.009	38.6098	11.5936	16.8099	17.3355
$h/2$	26624.8	4854.3	572.009	55.0266	2.06629	7.84921	8.44159
$h/4$	55119	6012.26	626.17	61.4406	2.28426	4.03192	4.66377
$h/8$	62527.3	6372	644.798	63.6811	4.41274	1.7983	2.43845
$h/16$	64019.3	6458.96	648.67	64.4924	5.56227	0.4704	1.08717
$\|\boldsymbol{u}_h - \boldsymbol{u}\|_1$							
h	82.4213	30.9496	5.3815	2.13908	2.11498	2.12159	2.12235
$h/2$	152.565	27.7869	3.43244	1.10907	1.0682	1.0702	1.07048
$h/4$	157.827	17.2204	1.86903	0.56062	0.53357	0.534409	0.534571
$h/8$	89.7451	9.14938	0.962713	0.280824	0.265866	0.266107	0.266215
$h/16$	46.0767	4.65057	0.485276	0.140333	0.132553	0.132565	0.13262

Results are shown for three choices of (γ, δ):

- $\gamma = -1$ and $\delta = -1$.
- $\gamma = 1$ and $\delta = -1$.
- $\gamma = -1$ and $\delta = 0$.

For all these cases, results are shown for several values for α ranging from 1 to 10^{-6}, as this stabilized Lagrange multiplier method is known to be stable only for a sufficiently small value of α. In some cases, especially when this seems to improve the convergence properties (for both velocity and pressure), results with larger values of α are also shown.

MINI-P_0. Tables 5–7 show the approximation errors using this combination of finite elements. All the results show convergence with an optimal linear rate for sufficiently small values of α. Moreover, with the choice $(\gamma, \delta) = (-1, -1)$, the numerical results also suggest that this formulation is stable whatever the value of the positive parameter α, even if for the largest values of α the convergence rate for the pressure seems suboptimal.

Table 8
Errors with the stabilized Lagrange multiplier method in the ring, using TH-P_1 elements, $\gamma = -1$, $\delta = -1$.

α	10^3	10^2	10^1	1	10^{-1}	10^{-2}	10^{-3}	10^{-4}	10^{-5}	10^{-6}
$\Vert p_h - p\Vert_0$										
h	11.1124	11.112	11.1077	11.0645	10.6463	8.05445	4.64999	3.90242	3.82317	3.81522
$h/2$	9.13573	9.13547	9.13281	9.10637	8.85213	7.14334	3.09731	1.42384	1.28167	1.27007
$h/4$	7.35829	7.35819	7.35726	7.34799	7.26333	6.72613	3.89165	0.960595	0.604564	0.597583
$h/8$	5.36342	5.3634	5.36327	5.36204	5.35877	5.57687	4.85624	1.38297	0.317426	0.301846
$h/16$	3.6321	3.63209	3.63199	3.63114	3.63273	4.03195	5.2358	2.32952	0.342948	0.149472
$\Vert \boldsymbol{u}_h - \boldsymbol{u}\Vert_1$										
h	9.64235	9.64236	9.64251	9.64417	9.67007	9.99932	10.6631	10.8515	10.874	10.8762
$h/2$	9.16379	9.1638	9.16388	9.16493	9.18837	9.65519	10.84	11.2271	11.2772	11.2823
$h/4$	8.13885	8.13885	8.13888	8.13936	8.15799	8.72026	10.6275	11.3354	11.435	11.4456
$h/8$	6.77044	6.77044	6.77045	6.77066	6.78353	7.32661	10.0507	11.3942	11.4931	11.5142
$h/16$	5.31468	5.31468	5.31468	5.31477	5.32218	5.72739	9.01859	11.1527	11.5022	11.5435

Table 9
Errors with the stabilized Lagrange multiplier method in the ring, using TH-P_1 elements, $\gamma = 1$, $\delta = -1$.

α	1	10^{-1}	10^{-2}	10^{-3}	10^{-4}	10^{-5}	10^{-6}
$\Vert p_h - p\Vert_0$							
h	511.276	442.435	159.638	11.5843	4.11762	3.83875	3.81672
$h/2$	2059.97	1806.5	692.163	35.1587	2.15667	1.32047	1.27361
$h/4$	6733.58	6007.04	2539.53	135.467	3.50774	0.685281	0.603186
$h/8$	18781.7	17057.6	8098.03	512.82	10.0292	0.565584	0.309791
$h/16$	46293.5	42676	22616.5	1841.03	33.3502	1.07646	0.171682
$\Vert \boldsymbol{u}_h - \boldsymbol{u}\Vert_1$							
h	13.8688	12.9557	10.4732	10.666	10.8518	10.874	10.8762
$h/2$	22.3074	20.061	11.8272	10.8455	11.2273	11.2772	11.2823
$h/4$	34.3053	30.8276	15.2947	10.6481	11.3354	11.435	11.4456
$h/8$	46.9802	42.7631	21.3396	10.13	11.3042	11.4931	11.5142
$h/16$	57.5357	53.0803	28.5675	9.30133	11.1528	11.5022	11.5435

Table 10
Errors with the stabilized Lagrange multiplier method in the ring, using TH-P_1 elements, $\gamma = -1$, $\delta = 0$.

α	1	10^{-1}	10^{-2}	10^{-3}	10^{-4}	10^{-5}	10^{-6}
$\Vert p_h - p\Vert_0$							
h	169.88	20.9785	10.0951	5.31388	3.97829	3.83085	3.81599
$h/2$	196.114	22.8672	13.8975	4.91088	1.6215	1.29956	1.27183
$h/4$	202.16	21.3463	21.6135	7.98238	1.45364	0.637933	0.60032
$h/8$	205.867	19.6504	30.6367	13.3808	2.43693	0.405724	0.305506
$h/16$	207.955	18.5673	38.706	21.4192	4.50048	0.571317	0.158353
$\Vert \boldsymbol{u}_h - \boldsymbol{u}\Vert_1$							
h	3.51333	4.48889	9.25317	10.6448	10.8514	10.874	10.8762
$h/2$	2.01106	2.58852	8.19593	10.7978	11.2267	11.2772	11.2823
$h/4$	1.03652	1.40852	6.47825	10.5423	11.3343	11.435	11.4456
$h/8$	0.527586	0.738418	4.52999	9.8916	11.302	11.4931	11.5142
$h/16$	0.266358	0.378667	2.82301	8.74975	11.1485	11.5022	11.5435

Taylor–Hood-P_1. Tables 8–10 show that whatever our three choices for (γ, δ), a convergence is very difficult to observe. This is particularly evident for small values of α as we observe that the velocity approximations do not converge at all. This is in contrast with the previous example with the same analytical solution in a polygonal domain Ω (a square), where convergence was observed with optimal (quadratic) rate. Note that when α is small, velocity approximations corresponding to different values of (γ, δ) seem to converge to the same limit. In Fig. 4 we see that the velocity approximation vanishes at the boundary corners of Ω_h, which makes us think that in theses cases Babuska's like paradox may be at play. The best convergent behavior seems to happen with $(\gamma, \delta) = (-1, -1)$ and moderate to large values of α (Table 8), but with a very suboptimal rate (just below 1/2 which is the rate obtained by Verfürth in [33]).

Taylor–Hood-P_0. We now use again Taylor–Hood finite elements for velocity and pressure, but this time combined with discontinuous P_0 instead of P_1 finite elements for the multiplier. We now obtain convergent approximations, for several choices of γ and δ, and for sufficiently small values of α (Tables 11–13). Convergence rates are not quadratic (between 1.5 and 2) but we do not expect them to be so, because of the error due to the approximation of Ω by Ω_h. Moreover, according to Theorem 1 we expect a linear convergence rate using P_0 finite elements for the multiplier. A possible explanation with the success of this combination of finite elements, compared to Taylor–Hood-P_1 elements, is that using P_0 elements instead

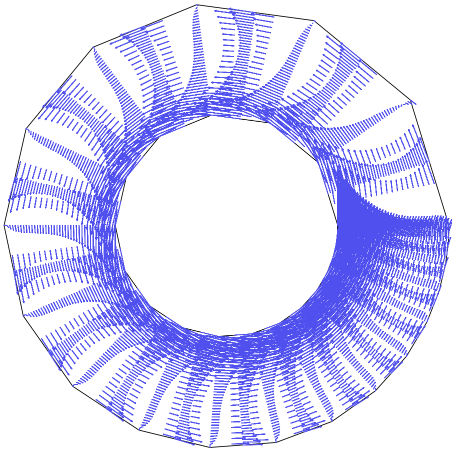

Fig. 4. Velocity field obtained with the stabilized Lagrange multiplier method formulation (18), with $\alpha = 10^{-6}$, and TH-P_1 finite elements.

Table 11
Errors with the stabilized Lagrange multiplier method in the ring, using TH-P_0 elements, $\gamma = -1$, $\delta = -1$.

α	1	10^{-1}	10^{-2}	10^{-3}	10^{-4}	10^{-5}	10^{-6}
$\Vert p_h - p\Vert_0$							
h	0.771038	0.767009	0.75627	0.748877	0.747541	0.747393	0.747378
$h/2$	0.177662	0.176388	0.173228	0.17248	0.172406	0.172397	0.172396
$h/4$	0.0444556	0.0438467	0.0423632	0.0421945	0.0421925	0.0421917	0.0421916
$h/8$	0.0115539	0.0112502	0.0104866	0.0103977	0.0103991	0.010399	0.010399
$h/16$	0.00315239	0.0030088	0.00262816	0.00257625	0.0025768	0.00257681	0.00257681
$\Vert \boldsymbol{u}_h - \boldsymbol{u}\Vert_1$							
h	0.65139	0.6441	0.620952	0.609931	0.608887	0.608795	0.608786
$h/2$	0.176529	0.172443	0.158909	0.153274	0.152965	0.152948	0.152947
$h/4$	0.0495436	0.0476224	0.040921	0.03810780	0.0379909	0.0379875	0.0379872
$h/8$	0.0147419	0.0139217	0.0108801	0.00950406	0.00945064	0.00944967	0.00944962
$h/16$	0.00465002	0.00432255	0.00303339	0.00238206	0.00235601	0.00235564	0.00235563

Table 12
Errors with the stabilized Lagrange multiplier method in the ring, using TH-P_0 elements, $\gamma = 1$, $\delta = -1$.

α	1	10^{-1}	10^{-2}	10^{-3}	10^{-4}	10^{-5}	10^{-6}
$\Vert p_h - p\Vert_0$							
h	29.1657	24.621	8.26168	0.933719	0.736062	0.745859	0.747221
$h/2$	36.1427	30.4328	10.0644	0.523726	0.171205	0.171836	0.172335
$h/4$	38.5329	32.5101	10.8177	0.465316	0.0449184	0.0420006	0.0421678
$h/8$	39.2827	33.1871	11.1009	0.461114	0.0147215	0.0103469	0.010389
$h/16$	39.5277	33.4188	11.2138	0.46432	0.00774521	0.00258201	0.00257248
$\Vert \boldsymbol{u}_h - \boldsymbol{u}\Vert_1$							
h	0.85374	0.793366	0.6374	0.60992	0.608888	0.608795	0.608786
$h/2$	0.39653	0.344902	0.186492	0.153311	0.152965	0.152948	0.152947
$h/4$	0.196833	0.167598	0.0672254	0.0381656	0.0379909	0.0379875	0.0379872
$h/8$	0.0983205	0.0832931	0.0295307	0.00956953	0.00945065	0.00944967	0.00944962
$h/16$	0.0491342	0.041579	0.0142022	0.0024497	0.00235602	0.00235564	0.00235563

of P_1 elements for the multiplier relaxes the constraint $\boldsymbol{u}_h \cdot \boldsymbol{\nu}_h = 0$ along each face of the polygonal boundary of Ω_h, allowing the velocity approximations not to vanish at boundary vertices. Note also that, if $(\gamma, \delta) = (-1, -1)$ (Table 11) or $(\gamma, \delta) = (-1, 0)$ (Table 13), convergence is observed whatever the value of α in the range 1 to 10^{-6}.

5.2.2. *Nitsche's method*

In this section we show the results of our computations with Nitsche's method (20) using MINI or TH finite elements. We consider two choices for (γ, δ):

- $\gamma = -1$ and $\delta = -1$.
- $\gamma = 1$ and $\delta = -1$.

Table 13
Errors with the stabilized Lagrange multiplier method in the ring, using TH-P_0 elements, $\gamma = -1$, $\delta = 0$.

α	1	10^{-1}	10^{-2}	10^{-3}	10^{-4}	10^{-5}	10^{-6}
$\Vert p_h - p\Vert_0$							
h	77.1065	7.54209	0.311522	0.671046	0.739677	0.746606	0.7473
$h/2$	34.8049	3.19183	0.193001	0.142837	0.169375	0.172093	0.172366
$h/4$	14.3248	1.31877	0.0995544	0.0306287	0.0409802	0.0420701	0.0421795
$h/8$	6.34711	0.582998	0.0501552	0.00577674	0.00987454	0.0103462	0.0103937
$h/16$	2.96311	0.271634	0.0251199	0.00126087	0.00233664	0.00255249	0.00257438
$\Vert \boldsymbol{u}_h - \boldsymbol{u}\Vert_1$							
h	1.65151	0.630616	0.609067	0.608794	0.608786	0.608785	0.608785
$h/2$	0.381181	0.156578	0.152984	0.152947	0.152946	0.152946	0.152946
$h/4$	0.0815651	0.0385965	0.0379932	0.0379872	0.0379872	0.0379872	0.0379872
$h/8$	0.0186169	0.00956785	0.0095079	0.00944963	0.00987454	0.00944962	0.00944962
$h/16$	0.0044304	0.00238122	0.00235588	0.00235563	0.00235563	0.00235563	0.00235563

Table 14
Errors with Nitsche's method in the ring, using MINI elements, $\gamma = -1$, $\delta = -1$.

α	10^4	10^3	10^2	10^1	1	10^{-1}	10^{-2}	10^{-3}	10^{-4}
$\Vert p_h - p\Vert_0$									
h	0.0584662	0.0580688	0.0551352	0.0474749	0.0413741	0.0393105	0.0389405	0.0388951	0.0388904
$h/2$	0.0119289	0.0120681	0.0132305	0.0164314	0.0146694	0.0122845	0.0117607	0.0116863	0.0116777
$h/4$	0.00311512	0.00321297	0.00420894	0.00933453	0.0111591	0.00868537	0.00795909	0.00785421	0.00784069
$h/8$	0.00105153	0.00104696	0.00123062	0.00479399	0.00869628	0.0062708	0.00511412	0.0049445	0.00492295
$h/16$	0.000839321	0.000816416	0.000638761	0.0021596	0.00676542	0.00505646	0.00321568	0.0029084	0.00287326
$\Vert \boldsymbol{u}_h - \boldsymbol{u}\Vert_1$									
h	5.22831	5.27024	6.1161	9.74844	11.2931	11.5119	11.5362	11.5387	11.539
$h/2$	3.02427	3.04363	3.74667	8.39182	11.0882	11.5075	11.5558	11.5609	11.5614
$h/4$	1.62553	1.63325	2.07622	6.56069	10.689	11.468	11.562	11.5721	11.5732
$h/8$	0.834657	0.837906	1.08467	4.56184	9.9681	11.3738	11.5542	11.5742	11.5762
$h/16$	0.421136	0.42261	0.552549	2.83407	8.7875	11.1919	11.5337	11.5727	11.5769

Table 15
Errors with Nitsche's method in the ring, using MINI elements, $\gamma = 1$, $\delta = -1$.

α	10^4	10^3	10^2	10^1	1	10^{-1}	10^{-2}	10^{-3}	10^{-4}
$\Vert p_h - p\Vert_0$									
h	0.560171	0.247249	2.08298	0.286255	0.0656897	0.0423473	0.0392188	0.0389224	0.0388932
$h/2$	2.09929	0.892728	0.280944	0.0968419	0.059324	0.0180836	0.0122159	0.011727	0.0116817
$h/4$	0.112048	0.8636	1.18376	0.231585	0.0642229	0.0197781	0.00871742	0.00790494	0.0078452
$h/8$	7.05268	1.7006	1.4314	0.39124	0.0507007	0.02642	0.00693521	0.00503181	0.00492816
$h/16$	1.68274	5.86637	0.578434	0.63682	0.0251573	0.0311573	0.0080579	0.00316844	0.00288234
$\Vert \boldsymbol{u}_h - \boldsymbol{u}\Vert_1$									
h	23.6071	20.842	58.9745	11.4169	11.2979	11.5128	11.5363	11.5388	11.539
$h/2$	43.0326	22.3998	14.4952	8.90433	11.0879	11.5076	11.5558	11.5609	11.5614
$h/4$	13.3703	23.5674	13.5654	7.03044	10.6864	11.468	11.562	11.5721	11.5732
$h/8$	65.9745	21.9374	19.3018	4.9529	9.96554	11.3737	11.5542	11.5742	11.5762
$h/16$	6.32842	26.6516	6.6403	4.94082	8.78569	11.1918	11.5337	11.5727	11.5769

Let us recall that, according to Proposition 2, formulation (20) with $(\gamma, \delta) = (-1, -1)$ is unconditionally stable while in the case $(\gamma, \delta) = (1, -1)$ it is known to be stable only if α is sufficiently small. This is why we perform the computations for values of α ranging from 1 to 10^{-4}. This range has proved to be sufficient to capture the convergence behavior for small values α. Additionally, computations are also performed with larger values of α, ranging from 1 to 10^4, for completeness.

According to Tables 14–17, whether with $\gamma = -1$ or $\gamma = 1$, and whether with MINI or TH elements, convergence of $(\boldsymbol{u}_h, p_h)$ does not seem to take place for small values of α, particularly for the velocity. As shown in Fig. 5, the velocity field approximations tend to vanish at vertices. On another hand, with large values α, the unconditionally stable formulation (that is with $(\gamma, \delta) = (-1, -1)$) combined with MINI or TH elements gives convergent approximations, although the convergence rate seems to deteriorate with increasing α. The best convergence rates (for both the pressure and the velocity) are observed for moderate values of α (in the range 10 to 10^2). Surprisingly, they are linear for MINI elements but lower with TH elements. For the conditionally stable formulation $((\gamma, \delta) = (-1, -1))$, it is difficult to find a condition on α that may indicate convergent approximations according to these numerical results.

Table 16
Errors with Nitsche's method in the ring, using TH elements, $\gamma = -1$, $\delta = -1$.

α	10^4	10^3	10^2	10^1	1	10^{-1}	10^{-2}	10^{-3}	10^{-4}
$\Vert p_h - p\Vert_0$									
h	0.0111135	0.0111204	0.011021	0.00834887	0.0037284	0.00248993	0.00235109	0.00233705	0.00233564
$h/2$	0.00913491	0.0091267	0.00900611	0.0074964	0.00314569	0.00110007	0.00103517	0.00104314	0.00104433
$h/4$	0.00735733	0.00734894	0.00728396	0.006879	0.00411366	0.000915148	0.000562492	0.000589486	0.000593725
$h/8$	0.0053623	0.00535298	0.00530912	0.00557822	0.00501116	0.00146635	0.000295468	0.000311115	0.000320417
$h/16$	0.0036307	0.00361901	0.00355999	0.00396453	0.0052913	0.00241058	0.000354037	0.000150636	0.000165784
$\Vert \boldsymbol{u}_h - \boldsymbol{u}\Vert_1$									
h	9.64193	9.63884	9.6442	9.99001	10.6665	10.8598	10.8858	10.8888	10.8891
$h/2$	9.16271	9.15413	9.13367	9.62858	10.8502	11.229	11.2804	11.2862	11.2868
$h/4$	8.13714	8.12331	8.07233	8.65267	10.644	11.3388	11.4357	11.4467	11.4478
$h/8$	6.76842	6.75181	6.67933	7.21239	10.0634	11.3122	11.4936	11.5145	11.5167
$h/16$	5.3127	5.29638	5.21846	5.58776	9.017	11.1643	11.5037	11.5436	11.5478

Table 17
Errors with Nitsche's method in the ring, using TH elements, $\gamma = 1$, $\delta = -1$.

α	10^4	10^3	10^2	10^1	1	10^{-1}	10^{-2}	10^{-3}	10^{-4}
$\Vert p_h - p\Vert_0$									
h	0.518906	0.508882	0.428803	0.14772	0.00996081	0.00250668	0.00233809	0.00233553	0.00233549
$h/2$	2.08765	2.05071	1.75042	0.634266	0.0333947	0.00174514	0.00103762	0.0010428	0.00104429
$h/4$	6.81056	6.69759	5.78699	2.29837	0.121298	0.00412763	0.000598173	0.000589642	0.000593724
$h/8$	18.958	18.662	16.3198	7.2397	0.444538	0.0112405	0.000683396	0.000311633	0.000320407
$h/16$	46.6511	45.9591	40.5935	19.9966	1.57753	0.0317202	0.00178028	0.000174324	0.000165643
$\Vert \boldsymbol{u}_h - \boldsymbol{u}\Vert_1$									
h	13.9749	13.8302	12.7547	10.3981	10.6691	10.86	10.8858	10.8888	10.8891
$h/2$	22.5563	22.2194	19.5435	11.4851	10.8554	11.2292	11.2804	11.2862	11.2868
$h/4$	34.6752	34.1284	29.7551	14.2895	10.6607	11.3389	11.4357	11.4467	11.4478
$h/8$	47.4119	46.6843	40.9436	19.3149	10.1231	11.3122	11.4936	11.5145	11.5167
$h/16$	57.9763	57.1221	50.5059	25.3683	9.22561	11.1644	11.5037	11.5436	11.5478

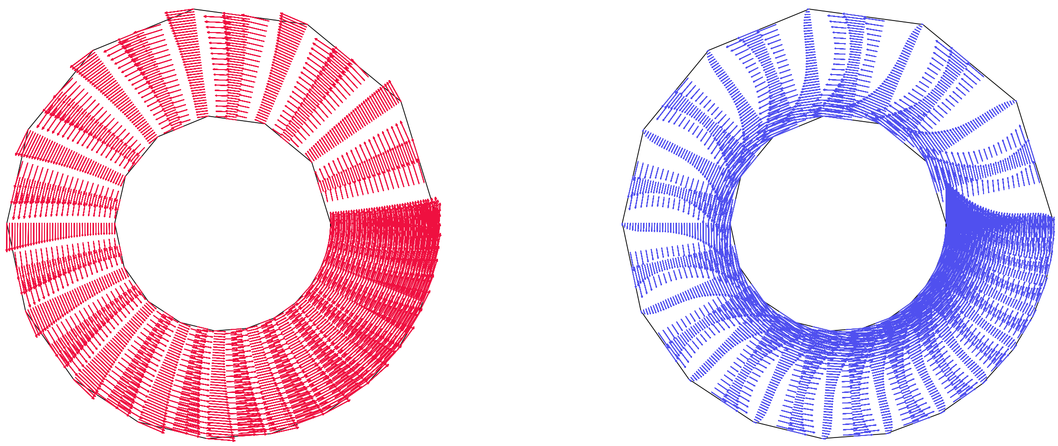

Fig. 5. Velocity field approximations using Nitsche's method and MINI element with $\gamma = -1$ and $\delta = -1$. Left: $\alpha = 10^3$. Right: $\alpha = 10^{-3}$.

6. Conclusion

In this paper we have studied, both theoretically and numerically, two methods to weakly impose the slip boundary condition for a viscous incompressible fluid, a stabilized formulation of the Lagrange multiplier method and Nitsche's method. For each method, there are several non-equivalent forms, depending on the values of a finite number of parameters. For the theoretical results, which extend previous results established by Verfürth [33] for the Lagrange multiplier method with a particular choice of the aforementioned parameters, we assume that the physical domain Ω has a polygonal or polyhedral boundary. Numerical results (in dimension 2) confirm the theoretical results for this category of domains.

For a domain having a smooth curved boundary (a ring), finite element approximations are computed in polygonal approximations Ω_h. Our numerical results indicate that, for both methods, convergence to the exact solutions may hold or not, depending on the finite element approximation spaces and on the values of the aforementioned parameters.

With the stabilized Lagrange multiplier method we recommend to use MINI-P_0 or TH-P_0 elements with small values of α and most of all with $\gamma = -1$ and $\delta = -1$, but not TH-P_1 elements. We also note that the case $\delta = 0$ corresponds to the variant analyzed by Verfürth. Our numerical results (Table 10) seem to contradict Verfürth's theoretical results in the case of TH-P_1 elements, except maybe with the value $\alpha = 10^{-1}$ although the convergence rate for the pressure is very low and from these results we cannot see how to recover a theoretically conforming convergence rate unless by taking unreasonably very small values of the element size h. The remaining results (Tables 7 and 13) are in agreement with his theoretical results.

Regarding Nitsche's method, MINI element worked well with the unconditionally stable formulation ($\gamma = -1$, $\delta = -1$) but only and surprisingly for moderately large values of α, and not at all with the conditionally stable one ($\gamma = 1$, $\delta = -1$). Using TH element gave at best very low convergence rates (for the unconditionally stable formulation with moderate to large values of α) and was unsuccessful with the conditionally stable formulation and whatever the value of α.

In cases where numerical convergence does not hold, a common feature is observed: velocity approximations almost vanish at the boundary vertices of Ω_h. This is not surprising since we tend to impose the velocity field to be parallel to each side of the polygonal boundary, thus to vanish at the common vertex of each pair of consecutive sides.

Let us note that several numerical remedies have been found and tested in order to circumvent Babuska's paradox in the finite element approximation of the plate equation with simple support boundary conditions. Let us mention, among them, the penalty method with reduced integration [10] and modified boundary conditions [27,10]. Similar remedies for Stokes equations with slip boundary conditions are presently under investigation by the authors of the present work. Finally, let us note that a similar study in three space dimension and associated remedies need to be investigated as well.

Acknowledgements

Authors are greatly indebted to Ibrahima Dione for his help with some of the figures.

Appendix A

A.1. Assumptions and proof of Proposition 1

For the proof of Proposition 1 and also Theorem 1, we make the following assumptions where $\mathcal{I}_h$, $\mathcal{J}_h$, and $\mathcal{K}_h$ are interpolation operators associated to V_h, Q_h and Λ_h respectively.

(H1) Classical LBB condition for Stokes equations (13): There exists $\beta > 0$ such that

$$\inf_{q\in Q_h} \sup_{\boldsymbol{v}\in V_h} \frac{\int_{\Omega_h} q\nabla\cdot\boldsymbol{v}\,d\Omega}{\|q\|_{0,\Omega_h}\|\boldsymbol{v}\|_{1,\Omega_h}} > \beta.$$

(H2) There exists $c_2 > 0$ such that

$$\|\boldsymbol{D}(\boldsymbol{v})\|_{0,S=\partial T\cap\Gamma_h} \leqslant c_2 h_S^{-1/2}\|\boldsymbol{D}(\boldsymbol{v})\|_{0,T}, \quad \forall T\in\mathcal{T}_h,\ \forall\boldsymbol{v}\in V_h.$$

(H3) There exists $c_3 > 0$ such that

$$\|p\|_{0,S=\partial T\cap\Gamma_h} \leqslant c_3 h_S^{-1/2}\|p\|_{0,T}, \quad \forall T\in\mathcal{T}_h,\ \forall\boldsymbol{v}\in V_h.$$

(H4) There exists $c_4 > 0$ such that

$$\|\boldsymbol{v}-\mathcal{I}_h(\boldsymbol{v})\|_{0,S=\partial T\cap\Gamma_h} \leqslant c_4 h_S^{1/2}\|\boldsymbol{v}\|_{1,T}, \quad \forall T\in\mathcal{T}_h,\ \forall\boldsymbol{v}\in V_h.$$

(H5) $\|\boldsymbol{v}-\mathcal{I}_h(\boldsymbol{v})\|_{m,T} \leqslant c_5 h_T^{l-m}, \|\boldsymbol{v}\|_{1,T}$, $\forall\boldsymbol{v}\in H^l(T)$, $0\leqslant m\leqslant 2$, $m\leqslant l\leqslant s+1$.
(H6) $\|\boldsymbol{v}-\mathcal{I}_h(\boldsymbol{v})\|_{0,S=\partial T\cap\Gamma} \leqslant c_6 h_T^{l+1/2}\|\boldsymbol{v}\|_{1,T}$, $\forall\boldsymbol{v}\in H^{l+1}(T)$, $0\leqslant l\leqslant s$.
(H7) $\|p-\mathcal{J}_h(p)\|_{m,T} \leqslant c_7 h_T^{l-m}\|p\|_{1,T}$, $\forall p\in H^l(T)$, $0\leqslant m\leqslant 1$, $m\leqslant l\leqslant s$.
(H8) $\|p-\mathcal{J}_h(p)\|_{0,S=\partial T\cap\Gamma} \leqslant c_8 h_T^{l-1/2}, \|p\|_{l,T}$, $\forall p\in H^l(T)$, $1\leqslant l\leqslant s$.
(H9) $\|\lambda-\mathcal{K}_h(\lambda)\|_{-1/2,S} \leqslant c_9 h_T^l\|\lambda\|_{l-1/2,S}$, $\forall\lambda\in H^{l-1/2}(S)$, $0\leqslant l\leqslant s$.
(H10) $\|\lambda-\mathcal{K}_h(\lambda)\|_{0,S} \leqslant c_{10} h_T^{l-1/2}\|\lambda\|_{l-1/2,S}$, $\forall\lambda\in H^{l-1/2}(S)$, $1\leqslant l\leqslant s$.

In the following, unless specified, $C, C_1, C_2, \ldots$ are generic constants which do not depend on α, δ or h. Let $(\boldsymbol{u}, p, \rho)\in V_h\times Q_h\times\Lambda_h$. Using Cauchy–Schwarz and triangular inequalities as well as assumptions (H2) and (H3) we obtain

$$\begin{aligned}
\mathcal{B}_{\alpha,h}\big((\boldsymbol{u},p,\rho),(\boldsymbol{u},-\gamma p,-\rho)\big) &= a_h(\boldsymbol{u},\boldsymbol{u}) + \alpha\|\rho\|^2_{-\frac{1}{2},h,\Gamma_h} + \alpha\langle\rho,\sigma(\boldsymbol{u},p)\rangle_{-\frac{1}{2},h,\Gamma_h} \\
&\quad - \alpha\delta\langle\rho+\sigma(\boldsymbol{u},p),\sigma(\boldsymbol{u},-\gamma p)\rangle_{-\frac{1}{2},h,\Gamma_h} \\
&\geqslant 2\mu\|D(\boldsymbol{u})\|^2_{0,\Omega_h} + \alpha\|\rho\|^2_{-\frac{1}{2},h,\Gamma_h} - \alpha\|\rho\|_{-\frac{1}{2},h,\Gamma_h} C_1\big(\mu\|D(\boldsymbol{u})\|_{0,\Omega_h} + \|p\|_{0,\Omega_h}\big)
\end{aligned}$$

$$
\begin{aligned}
&- \alpha|\delta|\big(\mu^2\big\|D(\boldsymbol{u})\big\|^2_{0,\Omega_h} + \|p\|^2_{0,\Omega_h}\big)\\
&\geqslant 2\mu\big\|D(\boldsymbol{u})\big\|^2_{0,\Omega_h} + \frac{\alpha}{2}\|\rho\|^2_{-\frac{1}{2},h,\Gamma_h} - \alpha C_1\big(\mu^2\big\|D(\boldsymbol{u})\big\|^2_{0,\Omega_h} + \|p\|^2_{0,\Omega_h}\big).
\end{aligned}
$$

In the right-hand side of the last inequality, the last term involving $D(\boldsymbol{u})$ can be controlled by the first one by choosing α sufficiently small. Let's assume for instance that

$$\alpha < \frac{1}{\mu C_1} \tag{24}$$

so that $\Delta_1 := 2\mu - \alpha C_1 > \mu$. We then obtain

$$\mathcal{B}_{\alpha,h}\big((\boldsymbol{u}, p, \rho), (\boldsymbol{u}, -p, -\rho)\big) \geqslant \Delta_1\big\|D(\boldsymbol{u})\big\|^2_{0,\Omega_h} + \frac{\alpha}{2}\|\rho\|^2_{-\frac{1}{2},h,\Gamma_h} - 2\alpha C_1\|p\|^2_{0,\Omega_h}. \tag{25}$$

On another hand, by definition of $H^{-1/2}(\Gamma)$, there exists $\boldsymbol{w} \in H^1(\Omega_h)$ such that

$$\langle\rho, \boldsymbol{w}\cdot\boldsymbol{\nu}\rangle_{\Gamma_h} = \|\rho\|^2_{-1/2,\Gamma_h}, \quad \text{and} \quad \|\boldsymbol{w}\|_{1,\Omega_h} = \|\rho\|_{-1/2,\Gamma_h}.$$

Note that we also have $\langle\rho, \boldsymbol{w}\cdot\boldsymbol{\nu}\rangle_{\Gamma_h} = b_{\Gamma_h}(\rho, \boldsymbol{w}\cdot\boldsymbol{\nu})$. Set $\boldsymbol{w_h} = \mathcal{I}_h(\boldsymbol{w})$. From assumptions (H2)–(H4) we obtain

$$
\begin{aligned}
\mathcal{B}_{\alpha,h}\big((\boldsymbol{u}, p, \rho), (\boldsymbol{w_h}, 0, 0)\big) &= a_h(\boldsymbol{u}, \boldsymbol{w}_h) + b_{\Omega_h}(\boldsymbol{w_h}, p) + b_{\Gamma_h}(\rho, \boldsymbol{w}\cdot\boldsymbol{\nu}) - b_{\Gamma_h}\big(\rho, (\boldsymbol{w} - \boldsymbol{w}_h)\cdot\boldsymbol{\nu}\big)\\
&\quad - \alpha\big\langle\rho + \sigma(\boldsymbol{u}, p), \delta\sigma(\boldsymbol{w}_h, 0)\big\rangle_{-\frac{1}{2},h,\Gamma_h}\\
&\geqslant -2\mu\big\|D(\boldsymbol{u})\big\|_{0,\Omega_h}\big\|D(\boldsymbol{w_h})\big\|_{0,\Omega_h} - \|p\|_{0,\Omega_h}\big\|D(\boldsymbol{w_h})\big\|_{0,\Omega_h}\\
&\quad + \|\rho\|^2_{-1/2,\Gamma_h} - \|\rho\|_{-\frac{1}{2},\Gamma_h}\|\rho\|_{-\frac{1}{2},h,\Gamma_h}\\
&\quad - \alpha|\delta|\|\rho\|_{-\frac{1}{2},\Gamma_h}\big(\|\rho\|_{-\frac{1}{2},h,\Gamma_h} + \mu\big\|D(\boldsymbol{u})\big\|_{0,\Omega_h} + \|p\|_{0,\Omega_h}\big)\\
&\geqslant \|\rho\|^2_{-1/2,\Gamma_h} - C_2(1+\alpha)\|\rho\|_{-\frac{1}{2},\Gamma_h}\big(\|\rho\|_{-\frac{1}{2},h,\Gamma_h} + \mu\big\|D(\boldsymbol{u})\big\|_{0,\Omega_h} + \|p\|_{0,\Omega_h}\big)\\
&\geqslant \frac{1}{2}\|\rho\|^2_{-1/2,\Gamma_h} - C_2\big(1+\alpha^2\big)\big(\|\rho\|^2_{-\frac{1}{2},h,\Gamma_h} + \mu^2\big\|D(\boldsymbol{u})\big\|^2_{0,\Omega_h} + \|p\|^2_{0,\Omega_h}\big).
\end{aligned} \tag{26}
$$

Moreover, from assumption (H1) there exists $\boldsymbol{v} \in V_0$ such that

$$\gamma b_{\Omega_h}(\boldsymbol{v}, p) \geqslant \beta\|p\|^2_{0,\Omega_h} \quad \text{and} \quad \|\boldsymbol{v}\|_{1,\Omega_h} = \|p\|_{0,\Omega_h}.$$

Note that $\boldsymbol{v}$ satisfies $\boldsymbol{v}_{|\Gamma_h} = 0$. Using these properties we easily obtain the estimate

$$
\begin{aligned}
\mathcal{B}_{\alpha,h}\big((\boldsymbol{u}, p, \rho), (\boldsymbol{v}, 0, 0)\big) &= a_h(\boldsymbol{u}, \boldsymbol{v}) + \gamma b_{\Omega_h}(\boldsymbol{v}, p) - \alpha\big\langle\rho + \sigma(\boldsymbol{u}, p), \delta\sigma(\boldsymbol{v}, 0)\big\rangle_{-1/2,h,\Gamma_h}\\
&\geqslant -2\mu\big\|D(\boldsymbol{u})\big\|_{0,\Omega_h}\big\|D(\boldsymbol{v})\big\|_{0,\Omega_h} + \beta\|p\|^2_{0,\Omega_h}\\
&\quad - \alpha|\delta|\big\|\sigma(\boldsymbol{v}, 0)\big\|_{-\frac{1}{2},\Gamma_h}\big(\|\rho\|_{-\frac{1}{2},h,\Gamma_h} + \mu\big\|D(\boldsymbol{u})\big\|_{-1/2,h,\Gamma_h} + \|p\|_{-1/2,h,\Gamma_h}\big)\\
&\geqslant \beta\|p\|^2_{0,\Omega_h} - 2\mu C_3\|p\|_{0,\Omega_h}\big\|D(\boldsymbol{u})\big\|_{0,\Omega_h}\\
&\quad - \alpha|\delta|C_3\|p\|_{0,\Omega_h}\big(\|\rho\|_{-\frac{1}{2},h,\Gamma_h} + \mu\big\|D(\boldsymbol{u})\big\|_{0,\Omega_h} + \|p\|_{0,\Omega_h}\big)\\
&\geqslant \frac{\beta}{2}\|p\|^2_{0,\Omega_h} - C_3\big(\alpha^2\|\rho\|^2_{-\frac{1}{2},h,\Gamma_h} + \big(1+\alpha^2\big)\mu^2\big\|D(\boldsymbol{u})\big\|^2_{0,\Omega_h}\big) - \alpha|\delta|C_3\|p\|^2_{0,\Omega_h}.
\end{aligned} \tag{27}
$$

In order to control the pressure terms, α needs again to be sufficiently small. Let's assume for instance that

$$\alpha < \frac{\beta}{4C_3} \tag{28}$$

so that $\Delta_3 = \beta/2 - \alpha C_3 > \beta/4$. This allows us to obtain

$$\mathcal{B}_{\alpha,h}\big((\boldsymbol{u}, p, \rho), (\boldsymbol{v}, 0, 0)\big) \geqslant \Delta_3\|p\|^2_{0,\Omega_h} - C_3\alpha^2\|\rho\|^2_{-\frac{1}{2},h,\Gamma_h} - C_3\big(1+\alpha^2\big)\mu^2\big\|D(\boldsymbol{u})\big\|^2_{0,\Omega_h}. \tag{29}$$

The remainder of the proof consists in taking a linear combination of (25), (26) and (29). Let us first introduce $m = \min\{1/\mu C_1, \beta/4C_3\}$. We assume that $0 < \alpha < m$ so that (24) and (28) are satisfied. For $a_3 > 0$, we have

$$
\begin{aligned}
\mathcal{B}_{\alpha,h}\big((\boldsymbol{u}, p, \rho), (\boldsymbol{u} + a_3\boldsymbol{v}, -\gamma p, -\rho)\big) &\geqslant \big(\Delta_1 - a_3C_3\big(1+\alpha^2\big)\mu^2\big)\big\|D(\boldsymbol{u})\big\|^2_{0,\Omega_h}\\
&\quad + \left(\frac{\alpha}{2} - a_3C_3\alpha^2\right)\|\rho\|^2_{-\frac{1}{2},h,\Gamma_h} + (a_3\Delta_3 - 2\alpha C_1)\|p\|^2_{0,\Omega_h}.
\end{aligned}
$$

Choosing a_3 sufficiently small, namely $a_3 < \min\{\Delta_1/C_3(1+m^2)\mu^2, 1/2C_3 m\}$ and taking $\alpha < a_3\beta/8C_1$ so that it satisfies $\alpha < a_3\Delta_3/2C_1$, this enables us to obtain

$$\mathcal{B}_{\alpha,h}\big((\boldsymbol{u},p,\rho),(\boldsymbol{u}+a_3\boldsymbol{v},-\gamma p,-\rho)\big) \geqslant C\big(\big\|D(\boldsymbol{u})\big\|^2_{0,\Omega_h} + \|\rho\|^2_{-\frac{1}{2},h,\Gamma_h} + \|p\|^2_{0,\Omega_h}\big).$$

It follows that

$$\begin{aligned}\mathcal{B}_{\alpha,h}\big((\boldsymbol{u},p,\rho),(\boldsymbol{u}+a_3\boldsymbol{v}+a_2\boldsymbol{w_h},-\gamma p,-\rho)\big) &\geqslant C\big(\big\|D(\boldsymbol{u})\big\|^2_{0,\Omega_h} + \|\rho\|^2_{-\frac{1}{2},h,\Gamma_h} + \|p\|^2_{0,\Omega_h}\big) + a_2\frac{1}{2}\|\rho\|^2_{-1/2,\Gamma_h} \\ &\quad - a_2 C_2\big(1+\alpha^2\big)\big(\|\rho\|^2_{-\frac{1}{2},h,\Gamma_h} + \mu^2\big\|D(\boldsymbol{u})\big\|^2_{0,\Omega_h} + \|p\|^2_{0,\Omega_h}\big).\end{aligned}$$

Choosing $a_2 > 0$ sufficiently small, we obtain a $(\boldsymbol{u_1}, q_1, \lambda_1) \in V_h \times Q_h \times \Lambda_h$ such that

$$\mathcal{B}_{\alpha,h}\big((\boldsymbol{u},p,\rho),(\boldsymbol{v_1},q_1,\lambda_1)\big) \geqslant C\big|\!\big|\!\big|(\boldsymbol{u},p,\rho)\big|\!\big|\!\big|^2_h, \tag{30}$$

As by construction we have $|||(\boldsymbol{v_1},q_1,\lambda_1)|||_h \leqslant C|||(\boldsymbol{u},p,\rho)|||_h$, the desired result is proved.

A.2. Proof of Proposition 2

Let $(\boldsymbol{u},p) \in V_h \times Q_h$. For both choices of δ, we have

$$\begin{aligned}\mathcal{D}_{\alpha,h}\big((\boldsymbol{u},p),(\boldsymbol{u},-\gamma p)\big) &= a(\boldsymbol{u},\boldsymbol{u}) + \frac{1}{\alpha}\langle \boldsymbol{u}\cdot\boldsymbol{\nu},\boldsymbol{u}\cdot\boldsymbol{\nu}\rangle_{\frac{1}{2},h,\Gamma} - b_\Gamma\big(\sigma(\boldsymbol{u},p),\boldsymbol{u}\big) - \delta\, b_\Gamma\big(\sigma(\boldsymbol{u},-\gamma p),\boldsymbol{u}\big) \\ &\geqslant 2\mu\big\|D(\boldsymbol{u})\big\|^2_{0,\Omega} + \frac{1}{\alpha}\|\boldsymbol{u}\cdot\boldsymbol{\nu}\|^2_{\frac{1}{2},h,\Gamma} \\ &\quad - \big(\big\|\sigma(\boldsymbol{u},p)\big\|_{-\frac{1}{2},h,\Gamma_h} + \big\|\sigma(\boldsymbol{u},-\gamma p)\big\|_{-\frac{1}{2},h,\Gamma_h}\big)\|\boldsymbol{u}\cdot\boldsymbol{\nu}\|_{\frac{1}{2},h,\Gamma}.\end{aligned}$$

Using (H2), (H4) and suitable triangular inequalities we deduce from the last inequality that

$$\mathcal{D}_{\alpha,h}\big((\boldsymbol{u},p),(\boldsymbol{u},-\gamma p)\big) \geqslant 2\mu\big\|D(\boldsymbol{u})\big\|^2_{0,\Omega} + \frac{1}{\alpha}\|\boldsymbol{u}\cdot\boldsymbol{\nu}\|^2_{\frac{1}{2},h,\Gamma} - c\varepsilon\big\|D(\boldsymbol{u})\big\|^2_{0,\Omega} - \frac{c\varepsilon}{\mu}\|p\|^2_{0,\Omega} - \frac{1}{\varepsilon}\|\boldsymbol{u}\cdot\boldsymbol{\nu}\|^2_{\frac{1}{2},h,\Gamma}.$$

On another hand, by (H1) there exists $\boldsymbol{v} \in \{v \in V_h\colon\ v_{|\Gamma_h} = 0\}$ such that $b_\Omega(\boldsymbol{v},p) \geqslant \beta\|p\|^2_{0,\Omega}$ and $\|D(\boldsymbol{v})\|_{0,\Omega} \leqslant \|p\|_{0,\Omega}$. Hence, again using (H2), (H3) and suitable triangular inequalities, we obtain

$$\begin{aligned}\mathcal{D}_{\alpha,h}\big((\boldsymbol{u},p),(\boldsymbol{v},0)\big) &\geqslant a(\boldsymbol{u},\boldsymbol{v}) + \beta\|p\|^2_{0,\Omega} - \delta b_\Gamma\big(\sigma(\boldsymbol{v},0),\boldsymbol{u}\big) \\ &\geqslant -2\mu\big\|D(\boldsymbol{u})\big\|_{0,\Omega}\big\|D(\boldsymbol{v})\big\|_{0,\Omega} + \beta\|p\|^2_{0,\Omega} - \big\|\sigma(\boldsymbol{v},0)\big\|_{-\frac{1}{2},h,\Gamma_h}\|\boldsymbol{u}\cdot\boldsymbol{\nu}\|_{\frac{1}{2},h,\Gamma_h} \\ &\geqslant -2\mu c\big\|D(\boldsymbol{u})\big\|_{0,\Omega}\|p\|_{0,\Omega} + \beta\|p\|^2_{0,\Omega} - c\|p\|_{0,\Omega}\|\boldsymbol{u}\cdot\boldsymbol{\nu}\|_{\frac{1}{2},h,\Gamma_h} \\ &\geqslant -4\frac{\mu^2}{\beta}\big\|D(\boldsymbol{u})\big\|^2_{0,\Omega} + \frac{\beta}{2}\|p\|^2_{0,\Omega} - \frac{c}{\beta}\|\boldsymbol{u}\cdot\boldsymbol{\nu}\|_{\frac{1}{2},h,\Gamma_h}.\end{aligned}$$

Let $\omega > 0$. Then

$$\begin{aligned}\mathcal{D}_{\alpha,h}\big((\boldsymbol{u},p),(\boldsymbol{u}+\omega\boldsymbol{v},-\gamma p)\big) &\geqslant \left(2\mu - c\varepsilon - 4\omega\frac{\mu^2}{\beta}\right)\big\|D(\boldsymbol{u})\big\|^2_{0,\Omega} + \left(\omega\frac{\beta}{2} - \frac{c\varepsilon}{\mu}\right)\|p\|^2_{0,\Omega} \\ &\quad + \left(\frac{1}{\alpha} - \frac{1}{\varepsilon} - \omega\frac{c}{\beta}\right)\|\boldsymbol{u}\cdot\boldsymbol{\nu}\|_{\frac{1}{2},h,\Gamma_h}.\end{aligned} \tag{31}$$

Choosing ω, ε and then α such that

$$\omega = \frac{\beta}{4\mu}, \qquad \varepsilon < \inf\left\{\frac{\mu}{c}, \omega\frac{\mu\beta}{2c}\right\} \quad \text{and} \quad \alpha < \frac{\beta\varepsilon}{\beta+\varepsilon\omega c}$$

respectively, we obtain

$$\mathcal{D}_{\alpha,h}\big((\boldsymbol{u},p),(\boldsymbol{u}+\omega\boldsymbol{v},q)\big) \geqslant C_1\big\|(\boldsymbol{u},p)\big\|^2_h \geqslant C_2\big\|(\boldsymbol{u},p)\big\|_h\big\|(\boldsymbol{u}+\omega\boldsymbol{v},p)\big\|_h,$$

for suitable $C_1, C_2 > 0$. Hence (22).

For the particular case where $\delta = -1$ and $\gamma = -1$, we have

$$\mathcal{D}_{\alpha,h}\big((\boldsymbol{u}, p), (\boldsymbol{u}, p)\big) = a(\boldsymbol{u}, \boldsymbol{u}) + \frac{1}{\alpha}\langle \boldsymbol{u}\cdot\boldsymbol{\nu}, \boldsymbol{u}\cdot\boldsymbol{\nu}\rangle_{\frac{1}{2},h,\Gamma_h}$$
$$= 2\mu\big\|D(\boldsymbol{u})\big\|^2_{0,\Omega} + \frac{1}{\alpha}\|\boldsymbol{u}\cdot\boldsymbol{\nu}\|^2_{\frac{1}{2},h,\Gamma_h},$$

so that the terms involving ε in (31) disappear. As a result, by simply choosing ω such that $\omega < \inf\{\frac{\beta}{c\alpha}, \frac{\beta}{2\mu}\}$ yields (22) without any condition on α other than $\alpha > 0$.

A.3. Proof of Theorem 2

From stability estimate (22) and consistency property (21), we obtain

$$\big\|(\boldsymbol{u}_h, p_h) - (\boldsymbol{v}_h, q_h)\big\|_h \leqslant C \sup_{(\boldsymbol{v}_h,q_h)\in V_h\times Q_h} \frac{\mathcal{D}_{\alpha,h}((\boldsymbol{u}_h, p_h) - (\boldsymbol{v}_h, q_h), (\boldsymbol{w}_h, r_h))}{\|(\boldsymbol{w}_h, r_h)\|_h}$$
$$\leqslant C \sup_{(\boldsymbol{v}_h,q_h)\in V_h\times Q_h} \frac{\mathcal{D}_{\alpha,h}((\boldsymbol{u}, p) - (\boldsymbol{v}_h, q_h), (\boldsymbol{w}_h, r_h))}{\|(\boldsymbol{w}_h, r_h)\|_h} \tag{32}$$

for all $(\boldsymbol{v}_h, q_h) \in V_h \times Q_h$. From the definition of $\mathcal{D}_{\alpha,h}$, applying Korn inequality (5) we obtain

$$\mathcal{D}_{\alpha,h}\big((\boldsymbol{u}, p) - (\boldsymbol{v}_h, q_h), (\boldsymbol{w}_h, r_h)\big) \leqslant \big(\big\|(\boldsymbol{u}, p) - (\boldsymbol{v}_h, q_h)\big\|_h + c_1\big\|\boldsymbol{\nu}.D(\boldsymbol{u} - \boldsymbol{v}_h).\boldsymbol{\nu}\big\|_{-\frac{1}{2},h,\Gamma_h} + c_2\|p - q_h\|_{-\frac{1}{2},h,\Gamma_h}\big)$$
$$\times \big(\big\|(\boldsymbol{w}_h, r_h)\big\|_h + c_3\big\|\boldsymbol{\nu}.D(\boldsymbol{w}_h).\boldsymbol{\nu}\big\|_{-\frac{1}{2},h,\Gamma_h} + c_4\,\|r_h\|_{-\frac{1}{2},h,\Gamma_h}\big). \tag{33}$$

Using (H2) and (H3) we obtain

$$\big\|(\boldsymbol{w}_h, r_h)\big\|_h + \big\|\boldsymbol{\nu}.D(\boldsymbol{w}_h).\boldsymbol{\nu}\big\|_{-\frac{1}{2},h,\Gamma_h} + \|r_h\|_{-\frac{1}{2},h,\Gamma_h} \leqslant c\big\|(\boldsymbol{w}_h, r_h)\big\|_h. \tag{34}$$

On the other hand, using the estimate

$$\|\phi\|^2_{0,\partial T} \leqslant c\left(h_T^{-1}\|\phi\|^2_{0,T} + h_T\|\phi\|^2_{1,T}\right) \tag{35}$$

which holds for sufficiently smooth $\boldsymbol{\phi} : \Omega_h \to \mathbf{R}$ (see [30]) we get

$$\big\|\boldsymbol{\nu}.D(\boldsymbol{u} - \boldsymbol{v}_h).\boldsymbol{\nu}\big\|_{-\frac{1}{2},h,\Gamma_h} + \|p - q_h\|_{-\frac{1}{2},h,\Gamma_h}$$
$$\leqslant c\big(\|\boldsymbol{u} - \boldsymbol{v}_h\|_{1,\Omega_h} + h\|\boldsymbol{u} - \boldsymbol{v}_h\|_{2,\Omega_h} + \|p - q_h\|_{0,\Omega_h} + h\|p - q_h\|_{1,\Omega_h}\big)$$

for sufficiently smooth $\boldsymbol{u}$ and p. Hence, combining (32), (33), (34) and (35) we obtain

$$\big\|(\boldsymbol{u}_h, p_h) - (\boldsymbol{v}_h, q_h)\big\|_h \leqslant C\big(\big\|(\boldsymbol{u}, p) - (\boldsymbol{v}_h, q_h)\big\|_h + h\,\|\boldsymbol{u} - \boldsymbol{v}_h\|_{2,\Omega_h} + h\,\|p - q_h\|_{1,\Omega_h}\big).$$

As a result of a triangular inequality and of interpolation properties (H5)–(H8), taking $\boldsymbol{v}_h = \mathcal{I}_h\boldsymbol{u}$ and $q_h = \mathcal{J}_h p$ we obtain

$$\big\|(\boldsymbol{u}_h, p_h) - (\boldsymbol{u}, p)\big\|_h \leqslant \big\|(\boldsymbol{u}_h, p_h) - (\boldsymbol{v}_h, q_h)\big\|_h + \big\|(\boldsymbol{u}, p) - (\boldsymbol{v}_h, q_h)\big\|_h$$
$$\leqslant (1 + C)\big\|(\boldsymbol{u}, p) - (\boldsymbol{v}_h, q_h)\big\|_h + Ch\big(\|\boldsymbol{u} - \boldsymbol{v}_h\|_{2,\Omega_h} + \|p - q_h\|_{1,\Omega_h}\big)$$
$$\leqslant Ch^\ell\big(\|\boldsymbol{u}\|_{\ell+1,\Omega_h} + \|p\|_{\ell,\Omega_h}\big),$$

for all $0 \leqslant l \leqslant s$.

References

[1] C. Amrouche, V. Girault, Decomposition of vector spaces and application to the Stokes problem in arbitrary dimension, Czechoslov. Math. J. 44 (1994) 109–140.

[2] I. Babuska, Stabilität des Definitionsgebietes mit Rücksicht auf grundlegende Probleme der Theorie des partiellen Differentialgleichungen auch in Zusammenhang mit der Elasticitätstheorie, Czechoslov. Math. J. 11 (1961) 76–105, 165–203.

[3] I. Babuska, The theory of small changes in the domain of existence in the theory of partial differential equations and its applications, in: Differential Equations and Their Applications, Academic Press, New York, 1963, pp. 13–26.

[4] E. Bänsch, K. Deckelnick, Optimal error estimates for the Stokes and Navier–Stokes equations with slip-boundary condition, Modél. Math. Anal. Numér. 33 (1999) 923–938.

[5] H.J.C. Barbosa, T.J.R. Hughes, Boundary Lagrange multipliers in finite element methods: error analysis in natural norm, Numer. Math. 62 (1992) 1–15.

[6] G.S. Beavers, D.D. Joseph, Boundary conditions at a naturally permeable wall, J. Fluid Mech. 30 (1967) 197–207.

[7] D.W. Bechert, M. Bruse, W. Hage, R. Meyer, Fluid mechanics of biological surfaces and their technological application, Naturwissenschaften 87 (2004) 157–171.

[8] F. Brezzi, M. Fortin, Mixed and Hybrid Finite Element Methods, Springer-Verlag, New York, 1991.

[9] E. Burman, P. Hansbo, A unified stabilized method for Stokes' and Darcy's equations, J. Comput. Appl. Math. 198 (2007) 35–51.
[10] M. Utku, G.F. Carey, Penalty resolution of the Babuska's circle paradox, Comput. Methods Appl. Mech. Eng. 41 (1983) 11–28.
[11] K.N. Christodoulou, L.E. Scriven, The fluid mechanics of slide coating, J. Fluid Mech. 99 (1992) 39–55.
[12] T. Clopeau, A. Mikelić, R. Robert, On the vanishing viscosity limit for the 2D incompressible Navier–Stokes equations with the friction type boundary conditions, Nonlinearity 11 (1998) 1625–1636.
[13] M.M. Denn, Issues in viscoelastic fluid mechanics, Annu. Rev. Fluid Mech. 22 (1990) 13–34.
[14] J. Douglas, J. Wang, An absolutely stabilized finite element method for the Stokes problem, Math. Comput. 34 (1989) 495–508.
[15] G. Fairweather, Finite Element Galerkin Methods for Differential Equations, Marcel Dekker, New York, 1978.
[16] L.P. Franca, R. Stenberg, Error analysis of some Galerkin least squares methods for the elasticity equations, SIAM J. Numer. Anal. 28 (1991) 1680–1697.
[17] J. Freund, R. Stenberg, On weakly imposed boundary conditions for second order problems, in: M. Morandi Cecchi, et al. (Eds.), Proc. 9th Int. Conf. Finite Elements in Fluids, Venice, 1995, pp. 327–336.
[18] P. Grisvard, Elliptic Problems in Nonsmooth Domains, Pitman, London, 1985.
[19] P. Hansbo, M.G. Larson, Discontinuous Galerkin methods for incompressible and nearly incompressible elasticity by Nitsche's method, Comput. Methods Appl. Mech. Eng. 191 (2002) 1895–1908.
[20] T.J.R. Hughes, L. Franca, A new finite element formulation for computational fluid dynamics: VII. The Stokes problem with various well-posed boundary conditions: symmetric formulations that converge for all velocity pressure spaces, Comput. Methods Appl. Mech. Eng. 65 (1987) 85–96.
[21] T.J.R. Hughes, L. Franca, M. Balestra, A new finite element formulation for computational fluid dynamics: V. Circumventing the Babuska–Brezzi condition: A stable Petrov–Galerkin formulation of the Stokes problem accommodating equal-order interpolation, Comput. Methods Appl. Mech. Eng. 59 (1986) 85–99.
[22] P. Knobloch, Variational crimes in a finite element discretization of 3D Stokes equations with nonstandard boundary conditions, East-West J. Numer. Math. 7 (1999) 133–158.
[23] V.G. Maz'ya, S.A. Nazarov, Paradoxes of limit passage in solutions of boundary value problems involving the approximation of smooth domains by polygonal domains, Math. USSR, Izv. 29 (1987) 511–533.
[24] B. Mohammadi, O. Pironneau, Analysis of the k–ϵ Turbulence Model, Wiley, 1974.
[25] C. Neto, D.R. Evans, E. Bonaccurso, H.-J. Butt, V.S.J. Craig, Boundary slip in Newtonian liquids: a review of experimental studies, Rep. Prog. Phys. 68 (2005) 2859–2897.
[26] J.A. Nitsche, Über ein Variationsprinzip zur Lösung von Dirichlet-Problemen bei Verwendung von Teilräumen, die keinen Randbedingungen unterworfen sind, Abh. Math. Semin. Univ. Hamb. 36 (1971) 9–15.
[27] R. Scott, A survey of displacement methods for the plate bending problem, in: K.-J. Bathe, J.T. Oden, W. Wunderlich (Eds.), Formulations and Computational Algorithms in Finite Element Analysis, MIT Press, Cambridge, 1977, pp. 855–876.
[28] R. Stenberg, On some techniques for approximating boundary conditions in the finite element method, J. Comput. Appl. Math. 63 (1995) 139–148.
[29] G. Strang, G.J. Fix, An Analysis of the Finite Element Method, 2nd ed., Wellesley-Cambridge Press, 2008.
[30] V. Thomée, Galerkin Finite Element Methods for Parabolic Problems, Springer, Berlin, 1997.
[31] R. Verfürth, Finite element approximation of steady Navier–Stokes equations with mixed boundary conditions, Modél. Math. Anal. Numér. 19 (1985) 461–475.
[32] R. Verfürth, Finite element approximation of incompressible Navier–Stokes equations with slip boundary conditions, Numer. Math. 50 (1987) 697–721.
[33] R. Verfürth, Finite element approximation of incompressible Navier–Stokes equations with slip boundary conditions II, Numer. Math. 59 (1991) 615–636.